Analyst

ROYAL SOCIETY OF CHEMISTRY

TUTORIAL REVIEW

View Article Online
View Journal | View Issue

Cite this: *Analyst*, 2022, **147**, 1777

Recent advances and applications to cultural heritage using ATR-FTIR spectroscopy and ATR-FTIR spectroscopic imaging

Guan-Lin Liu and Sergei G. Kazarian *

Scientific investigation of cultural heritage objects plays a vital role in a responsible modern approach to conservation and archaeology. Recent advances in spectroscopy, such as the development of Attenuated Total Reflection Fourier Transform Infrared (ATR-FTIR) spectroscopy and ATR-FTIR spectroscopic imaging, have opened up a window of opportunities for characterisation of materials in artefacts and collections from museums. This review summarises some of the recent advances and applications of these ATR-FTIR spectroscopic analytical techniques in the area of cultural heritage studies, including examples of cross-sections of oil paintings, paper, textiles, plastic objects, potteries, glasses and mineral artefacts. Two of the major advantages of ATR mode measurements are minimal or no requirements for sample preparation and its provision for high lateral spatial resolution. In addition to conventional single point detection, two-dimensional mapping and imaging is especially beneficial for chemical visualisation of multi-layered structure cultural objects. This review also explores the implications of these advantages as well as some limitations and provides a brief outlook for the possible future developments in this area.

Received 1st January 2022,
Accepted 27th March 2022

DOI: 10.1039/d2an00005a

rsc.li/analyst

Department of Chemical Engineering, Imperial College London, South Kensington Campus, London, SW7 2AZ, UK. E-mail: s.kazarian@imperial.ac.uk

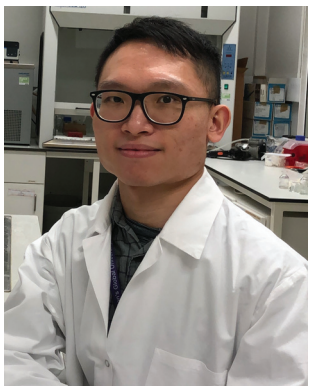

Guan-Lin Liu

Guan-Lin Liu obtained his MSc degree from the Department of Materials Science and Engineering at National Tsing Hua University in 2014. He has completed an MRes in Science and Engineering in Arts, Heritage and Archaeology at the University College London (UCL) in 2019. He is currently a PhD student in the Department of Chemical Engineering at Imperial College London. One of his main research interests is the development of new applications of ATR-FTIR spectroscopic imaging to heritage science and archaeometry.

Sergei G. Kazarian

*Sergei G. Kazarian is Professor of Physical Chemistry in the Department of Chemical Engineering at Imperial College London. His research encompasses the fields of vibrational spectroscopy, supercritical fluids, intermolecular interactions and materials. In the last two decades, his research has mainly been focused on developing and applications of spectroscopic imaging to materials, biomedical samples and pharmaceuticals (**https://www.imperial.ac.uk/vsci**). He also contributed to the fields of microfluidics, forensic science and analysis of materials of cultural heritage. He has published nearly 300 articles and reviews in leading scientific journals and he is Editor in Chief of Applied Spectroscopy. He presented his research at the Royal Society's 350th Anniversary Summer Science Exhibition in 2010 and he was awarded the RSC Sir George Stokes Award for his research with ATR-FTIR spectroscopic imaging in 2015.*

1. Introduction

Archaeometry, archaeological science[1] and conservation science[2] are research fields that utilise analytical methods to examine objects of cultural heritage or items in museum collections such as oil paintings, manuscripts, textiles, potteries and metallic artefacts for the purpose of understanding the original manufacturing techniques and materials, as well as tackling and solving problems concerning heritage conservation or preservation.[3] There are two main issues related to the preservation of cultural heritage, firstly, degradation which results from interaction between the materials used to produce the artworks, and secondly environmental influences such as light, heat and pollution. Conducting pre-emptive diagnosis measures will lead to effective, early identification of these problems and therefore prompt restoration of important objects of cultural heritage, leading to a time and cost reduction. Another problem is art fraud/forgery which must be recognised because forged copies may jeopardise authentic artworks. As a result, authentication is an important contribution to art history and curatorship.[4]

A wide variety of analytical techniques can be performed to investigate cultural heritage. Because of the uniqueness, value and significance of cultural heritage, the removal of cultural heritage for sampling and the damages caused by sample preparation should be as minimal as possible to minimise the loss of cultural heritage. Even in the case sampling is needed, it is beneficial that the sample can be left intact after the analysis because more information on this specific sample can be acquired by applying other complementary techniques. Non-invasive analysis requires no sampling, while non-destructive analysis need sampling but the sample is intact during analysis and thus available for future analyses. Non-invasive techniques, such as portable X-ray Fluorescence (XRF), X-ray radiography and portable UV/IR and Raman spectroscopy, are beneficial for scientific investigation of cultural heritage. These non-invasive techniques can also be employed *in situ*, offering identification of chemical heterogeneity of cultural heritage objects. Despite the usefulness of the non-invasive techniques, there are some limitations such as they are not able to provide detailed and/or stratigraphic characterisation of the samples.

Although it is ideal for the conservation field to adopt non-invasive approaches, there may be a fundamental need to obtain more unambiguous and detailed identification of the cultural heritage objects, the information which non-invasive approaches may not be sufficient to yield. As a result, micro-invasive analysis,[3,5] where a small amount of samples is extracted from cultural heritage objects using a micro-scale system, is necessary. Micro-invasive techniques can be non-destructive, allowing the samples to be intact for further study. The most common non-destructive analytical techniques that conservators and scientists employ in laboratories are Optical Microscopy (OM), Scanning Electron Microscopy (SEM) in combination with Energy Dispersion Spectroscopy (EDS), X-ray Diffraction (XRD) and Fourier Transform Infrared (FTIR) spectroscopy.

FTIR spectroscopy is an established analytical tool which has been applied to material identification of cultural heritage due to its sensitivity and specificity.[6] In recent decades, FTIR spectroscopic imaging systems have been developed which can obtain spatial and spectral information simultaneously, showing the chemical distribution over an area of the samples. Common FTIR spectroscopy and spectroscopic imaging techniques implemented to investigate cultural heritage and ancient artefacts include transmission, external reflection and Attenuated Total Reflection (ATR) mode.[7–9] This review focuses on the most recent advances in the field of ATR-FTIR spectroscopy and spectroscopic imaging to the investigation of objects of cultural heritage.

2. Fundamentals of ATR-FTIR spectroscopy and ATR-FTIR spectroscopic imaging

2.1 ATR-FTIR spectroscopy

There is an abundance of literature detailing infrared (IR) spectroscopy;[10–16] therefore in this review only some aspects are discussed. Both chemical and structural information from a sample can be acquired by identifying functional groups that have characteristic vibrational frequencies in the IR region. To investigate cultural heritage materials, the mid-IR range (4000–400 cm^{-1}) is commonly used.[17,18] In this region, most of the organic and inorganic materials which cultural objects are composed of can be identified with IR spectroscopy. Materials that have no vibrational modes in the mid-infrared region, such as certain sulphides and oxides, can be analysed using a far-infrared (FIR) detector as these materials may absorb in the far-IR region (400–50 cm^{-1}).[7,19]

One of the first papers using IR spectroscopy to investigate ancient artefacts was published in 1966.[17] Here, an improvement of spectral resolution and detection limit was noted due to the development of FTIR spectroscopy in place of dispersive IR; the former technique has contributed enormously to archaeometry and conservation of cultural heritage since 1980s.[18,20] As mentioned in the Introduction, FTIR spectroscopy typically utilises transmission, external reflection and ATR modes, as illustrated in Fig. 1 In a transmission measurement, infrared light passes through a sample, whilst in external reflection and ATR modes, the infrared light is reflected off the external or internal surfaces of the sample. External reflection and ATR are reflection modes which have simpler sample preparation compared to that for transmission mode requiring thin sections of samples which are generally between 3 and 10 μm to ensure that absorbance of all spectral bands is not out of scale. In an ATR measurement, the beam of infrared light is directed through an infrared transparent medium which has higher refractive index to the sample which has lower refractive index, but in an external reflection measurement, the infrared beam is not directed through the infrared transparent medium. This means that in ATR measurements,

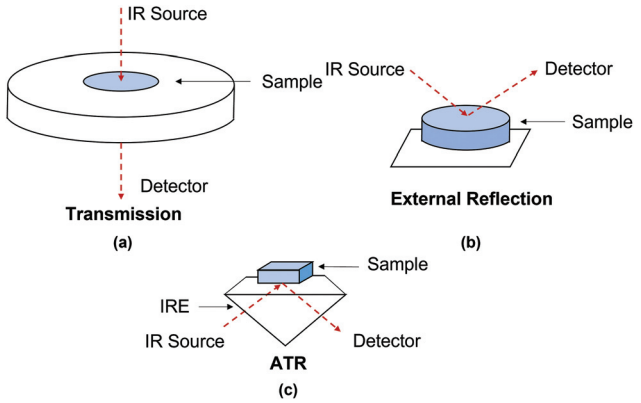

Fig. 1 Three typical modes of FTIR: (a) transmission, (b) external reflection and (c) ATR modes.

adequate contact between the IRE (see below) and the studied sample is necessary to achieve high-quality spectra.[21,22] In ATR measurements, absorption spectra are recorded, leading to no spectral distortion attributed from the variable contributions of both volume and surface reflection which can be seen in external reflection measurements.[23,24] As a result, spectral results produced by ATR-FTIR spectroscopy are comparable to that produced by transmission FTIR spectroscopy. However, a type of spectral distortions such as anomalous dispersion may happen in an ATR measurement when the angle of incidence close to the critical angle, particularly for samples with high refractive indices or when dispersion of the refractive index for samples is close to the wavelength of an absorbance band. As a result, this may cause significant shift in position of spectral band compared to the position of spectra band measured in transmission spectra. This minor problem may cause spectral misinterpretation if reference transmission mode spectra are directly used to explain acquired ATR spectra. In the authors' laboratory it has been demonstrated that it is possible to reduce the distortion of spectral bands by increasing angle of incidence, which significantly reduces the effect of anomalous dispersion. This approach was demonstrated in macro-ATR-FTIR spectroscopic imaging[25] as well as in micro ATR-FTIR spectroscopic imaging[26] which has been discussed in our review articles,[27,28] where the phenomenon of anomalous dispersion and the ways of its mitigating were presented in details.

In ATR-FTIR spectroscopy, an Internal Reflection Element (IRE) with a high refractive index (n_1) is brought into contact with an optically non-transparent sample which has a lower refractive index (n_2). IRE is often a hemi-sphere or a prism and most often made of diamond, silicon (Si), zinc selenide (ZnSe) or germanium (Ge). When the beam of IR is directed at above a certain angle, called the critical angle, total internal reflection occurs, where a standing wave of radiation called an evanescent wave is generated by IR light totally reflecting inside the IRE. This evanescent wave then interacts with the sample, attenuating the IR beam. The attenuated IR beam exits the IRE and reaches the detector, where the resulting signal is converted to an IR spectrum. The electric field of the evanescent wave exponentially decays to a distance from the surface of the IRE to e^{-1} of the maximum, which is known as the depth of penetration (dp) for non-absorbing materials. dp varies with the wavelength (λ), as shown in eqn (1). The penetration depth is also dependent on the angle of incidence of IR light and the refractive indices of both the sample and the IRE. The value of penetration depth is often within the range of 0.2–5 μm. Importantly, the electric field in ATR probes deeper than the dp, usually is about 3 times of dp. This probing effective thickness is defined by the thickness of a sample, when measured in transmission that would give the same absorbance for the same spectral band when compared to the ATR measurement.[29]

$$\mathrm{dp} = \frac{\lambda}{2\pi n_1 \sqrt{\sin^2\theta - \left(\frac{n_1}{n_2}\right)^2}} \quad (1)$$

2.2 ATR-FTIR spectroscopic imaging

An FTIR spectrometer coupled with an infrared array detector can be employed to simultaneously collect IR spectra and spatial locations within the sample, generating two-dimensional (2D) chemical images. These 2D chemical images indicate areas of high absorbance at a wavenumber for different materials over a region of the sample. Previously, these images where spectral and spatial information are acquired simultaneously were produced by point-by-point mapping using a single element detector, generally Mercury Cadmium Telluride (MCT). With the development of infrared array detectors, 2D chemical images can be obtained in more timesaving methods, such as line mapping and imaging[9] which both utilise multiple element detectors (usually MCT). The difference between the detectors of line mapping and imaging is that the line mapping detector is arranged in a linear array format, as known as Linear Array (LA), and the imaging detector is arranged in a square or rectangular array format, as known as Focal Plane Array (FPA), of which size is varied from 64 × 64, 128 × 128 to 256 × 256 elements (pixels). As a result, line mapping using LA enables spectra to be acquired through scanning rows of the static sample and then mapping into an image, whereas true imaging using FPA detector allows thousands of FTIR spectra from the whole sample area to be collected simultaneously into an image, thus allowing the studies of dynamic systems. Both methods have advantages and disadvantages which are not discussed in this paper but can be referred to elsewhere.[27,30] Illustration of these three different methods for producing 2D chemical images is shown in Fig. 2.

ATR-FTIR spectroscopic imaging using an FPA detector can be operated in two modes: micro and macro. The micro setup utilises a microscope to spatially locate the detected area of the sample. In addition, the IRE used in the micro mode is often a Ge crystal which provides a high lateral spatial resolution. The lateral spatial resolution (in this paper we ignore axial resolution and refer only lateral resolution to spatial

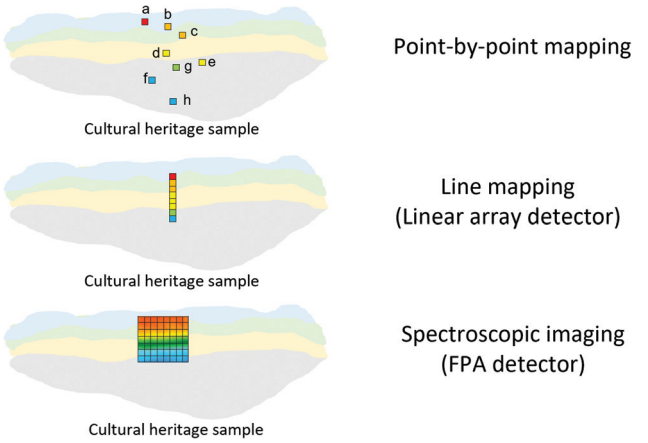

Fig. 2 Schematic of point-by-point mapping, line mapping and spectroscopic imaging. The colours of pixels represent concentration of an investigated component. Red/orange colours represent a high concentration of the component while blue/green region shows a low concentration.

resolution), defined as the minimum distance between two distinguishable points, is restricted by the diffraction limit as shown in eqn (2):

$$r = \frac{0.61\lambda}{\mathrm{NA}} \quad (2)$$

(where NA is the numerical aperture of the objective which is defined as $n\sin(\alpha)$ where n is the refraction index of the imaging medium between the objective and the sample and α is half the angular aperture).

Micro ATR-FTIR spectroscopic imaging provides high lateral spatial resolution because of much higher numerical aperture (n for Ge = 4). Compared to the micro setup, the macro setup is performed without using a microscope and the IRE used in the macro mode is an inverted prism that can be made of ZnSe, Ge, Si, and diamond. The IRE is installed on an ATR accessory in a large sample compartment that connects to an FTIR spectrometer. Macro ATR-FTIR imaging offers possibilities for scanning large sample areas consisting of a complex heterogeneous matrix. Table 1 summarises the different measurement fields of view and the lateral spatial resolutions using different ATR imaging accessories from the authors' laboratory.[31,32] ATR-FTIR spectroscopic imaging in its macro and micro modes has been applied to a wide variety of research field ranging from biological systems,[33] polymers,[34] pharmaceutics[35] and forensic science.[36] There is a perception among some researchers that pressure required to achieve a good contact may cause damage on the cultural heritage sample. Therefore, ATR-FTIR spectroscopic imaging cannot be considered a non-destructive technique. However, from the experience of the authors' laboratory, a good contact can be achieved without the need to apply much pressure and thus would not damage the sample or leave a mark. In ATR-FTIR spectroscopic imaging it is possible to observe the quality of contact of Ge crystal with the sample in live touching using FPA detector and to measure the smallest pressure for taking measurements.

Table 1 Measurement parameters of different ATR-FTIR spectroscopic imaging accessories. Reprinted with permission,[31] copyright (2017) The Royal Society of Chemistry

ATR accessory	Image size	Lateral spatial resolution[a]
Germanium micro ATR crystal in a microscope objective	64 μm × 64 μm	4 μm
Zinc selenide crystal (Oil Analyzer, Specac Ltd) in macro ATR imaging	2.5 mm × 3.6 mm	40 μm
Diamond crystal (Golden Gate, Specac Ltd) in macro ATR imaging	500 μm × 700 μm	15 μm

[a] Lateral spatial resolution is estimated based on using a wavenumber of 1700 cm^{-1}.

Various types of cultural heritage can be characterised for molecular analysis using ATR-FTIR spectroscopic mapping and imaging. Cultural objects which have multi-layered structures or are polychrome, such as oil paintings, historical paper and polychrome sculptures, are typical examples. These multi-layered structures of cultural heritage may be composed of heterogeneous mixtures of organic/inorganic materials and possible deterioration products. ATR-FTIR spectroscopic mapping and imaging can offer identification and spatial location of these various components of cultural heritage, contributing to addressing specific analytical issues and conservation problems. The recent applications of using ATR-FTIR spectroscopic mapping and imaging are highlighted in Section 3.

2.3 Sample preparation

As discussed in Section 2.1, commonly used acquisition modes for investigation of cultural heritage include external reflection, ATR and transmission. The choice of acquisition modes depends on the type, nature and amount of available samples and the research questions. Sampling, which is the process of extracting a small portion of material for further analysis, is often necessary for ATR-FTIR spectroscopic analyses. Because of the fragile state, the preciousness and the aesthetic properties of cultural heritage objects, lower amount of sampling is preferred. Micro-sampling[3] which requires small amount of the material (~100 μm^2 or ~0.05–0.1 g, dry weight) to be taken can be used for ATR-FTIR spectroscopic measurements because of its high sensitivity and specificity. Micro sampling may reduce or even avoid noticeable damages to cultural heritage objects. Furthermore, samples taken from cultural heritage objects can be measured repeatedly using this non-destructive ATR-FTIR spectroscopic technique and other non-destructive analytical equipment.

Powder and fragments are common types of samples for the analysis in ATR-FTIR spectroscopic measurements. Fragments contain cross-section and thin-section approaches which work in reflection and transmission mode, respectively. As mentioned in Section 2.1, thin sections which generally require thicknesses of samples to be between 3–10 μm is a

more difficult sample preparation, especially for investigating complex artwork stratigraphy samples. Therefore, cross sections are more commonly prepared. Sample preparation of both cross and thin sections is conducted by immersing a fragment sample in an embedding material as support which hardens in a short period of time. These embedding materials are often organic polymers such as polyester resins or acrylate.[37] However, these organic polymers might permeate into the sample fragments, causing acquisition of spectral signal of the polymers that impede the IR bands of the sample fragments. This problem can be solved using alternative IR-transparent salts such as silver chloride (AgCl) or potassium bromide (KBr).[38–41] The spectral interferences caused by polyester resins or acrylate can be eliminated with these alternative IR-transparent salts. Nonetheless, AgCl encounters darkening and accelerated corrosion problems. Also, KBr is a hygroscopic salt that causes unfeasible preservation for the fragment sample and reduces spectral quality shortly after sample preparation. Moreover, because KBr is more fragile than organic polymers, when a polishing procedure is needed it may lead to damage to the sample. Other feasible approaches may be coating the sample with cyclododecane ($C_{12}H_{24}$) before the sample is embedded in the organic polymer. This approach avoids penetration of the organic polymers into the sample,[42,43] but cyclododecane sublimates at room temperature, leaving a gap between the sample and the embedding material. This gap may cause non-optimal sample-ATR crystal (IRE) contact when conducting ATR measurements, leading to poor spectral quality. Furthermore, depending on the roughness of the sample it is not always possible to obtain adequate contact between the IRE of ATR and the sample. There are ways to overcome such challenge by using an immersion medium on the cross-sections of different samples of objects of cultural heritage embedded in polyester resin. For example, adding droplet of water to fill air gaps allows us to obtain high quality spectra from the paint cross-sections and successfully localise either inorganic compounds or organic substances present as painting materials studied by macro ATR-FTIR spectroscopic imaging.[22]

3. Fields of application for cultural heritage analysis using ATR-FTIR spectroscopy and ATR-FTIR spectroscopic imaging

3.1 Multi-layered painted artworks

3.1.1 FTIR spectra of materials used for multi-layered painted artworks. FTIR spectroscopy is an ideal tool to examine oil paintings because the paintings consist of multiple layers, which have a variety of organic and inorganic components that can be identified with FTIR spectroscopy or spectroscopic imaging. Typically, an oil painting may be layered with varnish, glazing, paint layer, underpainting, underdrawing, ground, canvas and wooden stretcher, from the top to the bottom. Among these layers, especially the upper layers, pigments, fillers and binders are often investigated and identified using FTIR spectroscopy and Raman spectroscopy. Both organic and inorganic pigments in paintings have been studied extensively.[44–49] The inorganic pigments have metal elements which can be detected with XRF. However, details such as complex structures of these pigments can only be further investigated with FTIR spectroscopy and Raman spectroscopy. Databases of these inorganic materials used in paintings have been studied and built.[49,50] Compared to inorganic pigments, organic pigments may have more complex IR spectra and are more likely to suffer from degradation, especially photochemical degradation due to light exposure.[51] Metal Underlayer Attenuated Total Reflection (MU-ATR) spectroscopy which is an enhanced sensitivity spectroscopic technique has been employed to investigate organic pigments by analysing a few ng of samples.[52] This new enhanced FTIR method can reduce the amount of samples, which can be promising for the analysis of trace amount of organic pigments in paintings or textiles. The detailed analytical procedure and applications of MU-ATR-FTIR spectroscopy are described elsewhere.[52–54] Identification of pigments is of importance because it can provide early detection of degradation and prompt conservation, and also interpretation of the techniques and palette of artists.

Binders used in paintings have been greatly characterised using FTIR spectroscopy.[55] Widely used binders are egg tempera, linseed oil, gum arabic and animal glue. The purpose of using these binders in the painting is to mix with organic/inorganic pigments powders, maintaining uniform pigments. It is worth noticing that there may be overlap in spectra between these different binders in complex paint samples. For example, both egg tempera and linseed oil contain triglycerides which have C–H stretching bands at around 2923 and 2872 cm^{-1}, so it may be difficult to distinguish these two binders when interpreting spectra. However, egg tempera also contain protein, so two strong characteristic bands at around 1650 cm^{-1} (amide I, C=O stretching) and 1550 cm^{-1} (amide II, N–H bending) can be used to identify the egg. The FTIR spectroscopic results can be supported and strengthened in combination with a more complete characterisation using Gas Chromatography-Mass Spectrometry (GC-MS), which provides qualitative and quantitative analysis of different analytes.[56,57]

Vahur *et al.* has contributed to building ATR-FTIR spectral databases of materials used in paintings including paint materials (inorganic pigments, fillers, binders), oil paints and protective coatings.[58–60] These databases can be freely searched online.[58] In these databases, the IR region is extended to include mid-IR and far-IR region. Painting materials are often complex mixed organic and inorganic components which may have similar or overlapped characteristic bands in the mid-IR region, leading to difficult identification. This problem can be solved by examining spectral

bands in the far-IR region. Most organic constituents such as ester and proteins have spectral bands in the mid-IR region but have no absorption in the far-IR region, while some inorganic substances have absorption in both mid-IR and far-IR regions. Therefore, by examining spectral bands in the far-IR region these inorganic substances can be identified.[58]

3.1.2 Case studies: paintings. For investigation of oil paintings, non-invasive techniques such as analytical single point devices (*e.g.* Fibre Optic Reflectance Spectroscopy (FORS) as well as hyperspectral imaging systems in visible and Near-Infrared (NIR) regions) have been exploited to analyse original materials, retouching and degradation.[61–63] Although these techniques are non-invasive and can be used to discriminate chemical components in the paintings, their spectra are often hard to interpret and needs further confirmation using other analytical techniques such as Raman and FTIR spectroscopies.[64] More detailed information can be acquired by examining the stratigraphy of paintings. Non-invasive approaches such as Optical Coherence Tomography (OCT),[65] Nuclear Magnetic Resonance (NMR),[66] Terahertz imaging,[67] confocal XRF[68,69] and micro-Spatially Offset Raman Spectroscopy (micro-SORS)[69] can be performed to investigate and characterise the layer successions, but they are not able to provide the two-dimensional distribution of compositional information of the materials. ATR-FTIR spectroscopy can be combined with multivariate techniques to analyse spatial and compositional information of the stratigraphy of a painting.[42,70] It is of great importance to obtain stratigraphic component information to clarify the original manufacturing technique, deterioration phenomena and subsequent restoration history of the painting. For example, a wall painting may be fresco or secco that can be hard to determine with the naked eye. The main difference between these two types of wall paintings is that the binders of fresco and secco are inorganic and organic compounds respectively. Furthermore, in fresco, calcium hydroxide solution (lime water paste) was added to mix with pigments of the wall paintings.[71,72] ATR-FTIR spectroscopy can be used to confirm whether the fresco or secco technique was used in the manufacturing of wall paintings by detecting the binder areas.[71,73]

Metal carboxylates, as known as metal soaps, are a typical deterioration problem in paintings. This problem is caused by the interaction between metal ions from pigments and fatty acids from binders.[74] Metal carboxylates might be protrusions on the surface of paintings or aggregated crystals between paint layers. These two forms of deterioration product, protrusions and aggregated crystals, would either affect aesthetical and structural properties of the paintings.[74–76] Issues of metal carboxylates have been fully explored and discussed in a comprehensive book.[77] Micro ATR-FTIR spectroscopic imaging has been used for the first time to identify metal soaps owing to COO^- bands in studies by Spring *et al.*[78] High lateral spatial resolution of micro ATR-FTIR spectroscopic imaging allows to resolve layers of a few micrometres in the samples from the corresponding paintings and thus reveal the chemical distribution and identify degradation process of metal soaps.[75] The use of Synchrotron Radiation (SR) sources for FTIR spectroscopic techniques can increase signal to noise in obtained spectra and improve spatial resolution in mapping approaches.[79,80] However, it is often preferred conducted in transmission mode which requires thin-section preparation, making sampling more challenging. ATR-FTIR spectroscopy has been used to distinguish different metal soaps by examining the positions of COO^- bands with different metal ions which are shifted to different frequencies.[81] Metal ions that interact with fatty acid forming metal soaps such as zinc,[82–84] copper,[78,85] lead,[78,86] cadmium and chromium[87] have been examined using ATR-FTIR spectroscopic mapping and imaging. To confirm metal ions more precisely in the metal carboxylates, SEM-EDX is often employed. Fig. 3 shows an example of chemical characterisation of a white paint cross-section from Jackson Pollock's *Alchemy* (1947).[75] ATR-FTIR 2D chemical images and SEM-EDX elemental images are reported to indicate the distribution of metals (Al, Zn and Ti) and location of Zn carboxylates, $ZnSt_2$ and $AlSt(OH)_2$, featuring the band at 1590 cm^{-1}, 1540 cm^{-1} and 1588 cm^{-1}, respectively. Another research using SEM-EDX and ATR-FTIR imaging, where pigments, extenders and binding media were identified in the stratigraphy of a painting claimed to be painted by Vincent van Gogh, detected deterioration products such as cadmium oxalate and zinc palmitate/stearate for the first time.[88] In addition to the identification of painting materials and deterioration products, ATR-FTIR spectroscopic imaging is also a powerful technique to study the formation of metal soaps by discussing dynamic processes of fatty acid and metal diffusion.[89,90] In conservation or restoration of paintings, it is important to discuss cleaning solvent diffusion and paint swelling. Time-resolved ATR-FTIR spectroscopy can accurately monitor diffusion and swelling processes.[90] The chemical composition of polymer materials that are used in restoration works have been researched using ATR-FTIR spectroscopy.[91] Recently, chemometric methods such as Partial Least Squares (PLS) or Orthogonal Partial Least Squares (OPLS) have been utilised in conjunction with ATR-FTIR spectroscopy to quantify pigments and coatings[92] and estimate ages of paints.[93]

3.1.3 Case studies: other cultural heritage subject to metal soaps. Apart from oil paintings, micro ATR-FTIR imaging can also be utilised for investigation of other artefacts consisting of oil-based paint materials that are subjected to saponification. Fig. 4 shows the identification of organic and inorganic substance distributions in the cross-sectional layer of a cold painted terracotta statue[94] using micro ATR-FTIR spectroscopic imaging. Demonstrated by the ATR-FTIR spectroscopic images, a complex sequence of 7 layers can be observed in the painted materials on the terracotta statue. The ATR-FTIR images are acquired by plotting the integrated spectral bands of each substance summarised in Table 2. The distributions of these substances in the chemical images contribute to the chemical identification of pigments, binders and deterioration products (protrusions) and shed light on a possible cause of the for-

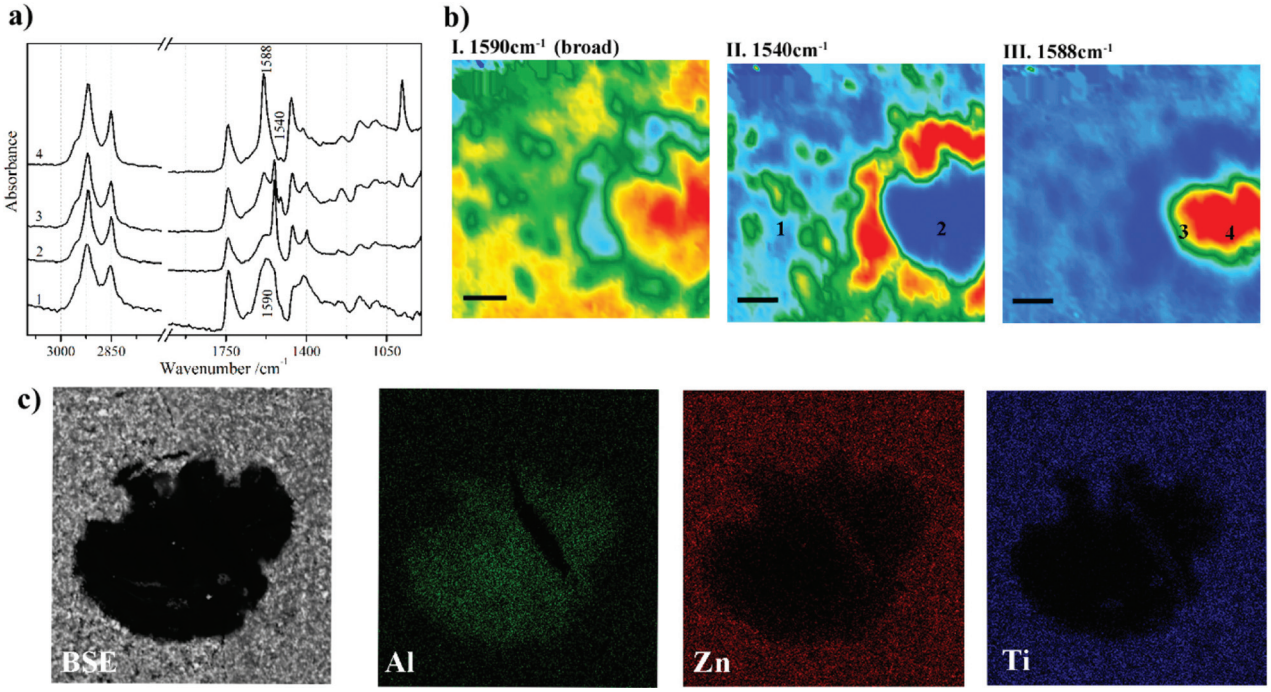

Fig. 3 Chemical characterisation of a white paint cross-section from Jackson Pollock's *Alchemy* (1947). (a) Extracted ATR-FTIR imaging spectra corresponding to four locations in (b) chemical images of the cross section. The chemical images are acquired by plotting the integrated absorbance at 1590, 1540 and 1588 cm^{-1}, which are characteristic bands of Zn carboxylates, $ZnSt_2$ and $AlSt(OH)_2$, respectively. (c) SEM and EDX images of the metal soaps in the cross section. Reprinted with permission,[75] copyright (2016) American Chemical Society.

mation of metals soaps. In a separate study, samples of cross-sections from terracotta altar-piece were studied with the greater field of view using macro ATR-FTIR spectroscopic imaging, where the composition of complete stratigraphy was obtained.[22]

As discussed above, metal soaps formed in paintings or oil-based painted materials are due to the reaction between metal ions from pigments and fatty acids from organic binders. Nevertheless, metal soaps can occur in other cultural heritage samples as a result of a mixture of metal ions and fatty acids. Leather is one of the striking examples where metal soaps are formed because a combination of metal oxide and fat residue remained on the skin during the manufacturing process. The mechanism of these metal soaps can be investigated using macro ATR-FTIR imaging. In a case study of 17th and 18th century leather book covers from Armenia,[95] ATR-FTIR spectroscopic images indicate the formation mechanism of calcium stearates which is a kind of calcium soaps, as shown in Fig. 5. The formation mechanism of Ca soaps (saponification) can be explained by quantitative analysis of Ca soaps with regard to calcium carbonate ($CaCO_3$) and gypsum ($CaSO_4{\cdot}2H_2O$) by looking at the spatial distribution of stearate, carbonate and gypsum in the ATR-FTIR images. In the spectra of the selected consecutive five pixels from the ATR-FTIR images, the absorbance of stearate increases as the absorbance of the carbonate and sulphate decreases. The spatial distribution and spectral variation analyses using ATR-FTIR imaging offer the evidence of saponification of original $CaCO_3$ and gypsum in the leather book covers.

3.2 Paper

3.2.1 FTIR spectra of paper materials. The main constituent of paper is cellulose, which is a polysaccharide composed of a linear chain of D-glucose units. These D-glucose units are linked by β-(1,4)-glycosidic bonds and the number of the D-glucose in cellulose can be hundreds to thousands.[96,97] In FTIR spectra of paper, a strong and broad band at around 3330 cm^{-1} attributed to O–H stretching vibration of H-bonded hydroxyl groups can be observed.[98,99] Other typical bands in the spectra of paper cellulose includes bands at 2900 cm^{-1} (C–H stretching), 1630 cm^{-1} (H_2O molecule absorption), 1428 cm^{-1} (CH_2 bending), 1367 cm^{-1} (CH bending), 1028 cm^{-1} (C–O stretching) and 897 cm^{-1} (C–O–C stretching).[100–103] Among these typical bands, the band at 1428 cm^{-1} is correlated to the crystallinity of cellulose, whereas the band at 897 cm^{-1} is associated with the amorphous zones in cellulose.[104] Nelson and O'Connor[105] proposed an IR crystallinity index determined by the ratio between the bands at 1428 cm^{-1} and 897 cm^{-1}. This calculated index using FTIR spectra has been employed to analyse changes in cellulose crystallinity by a great amount of research.[103,106,107]

In addition to cellulose, other components to manufacture paper might include organic and/or inorganic matters such as hemicellulose, lignin, clay, kaolin, titanium dioxide (TiO_2),

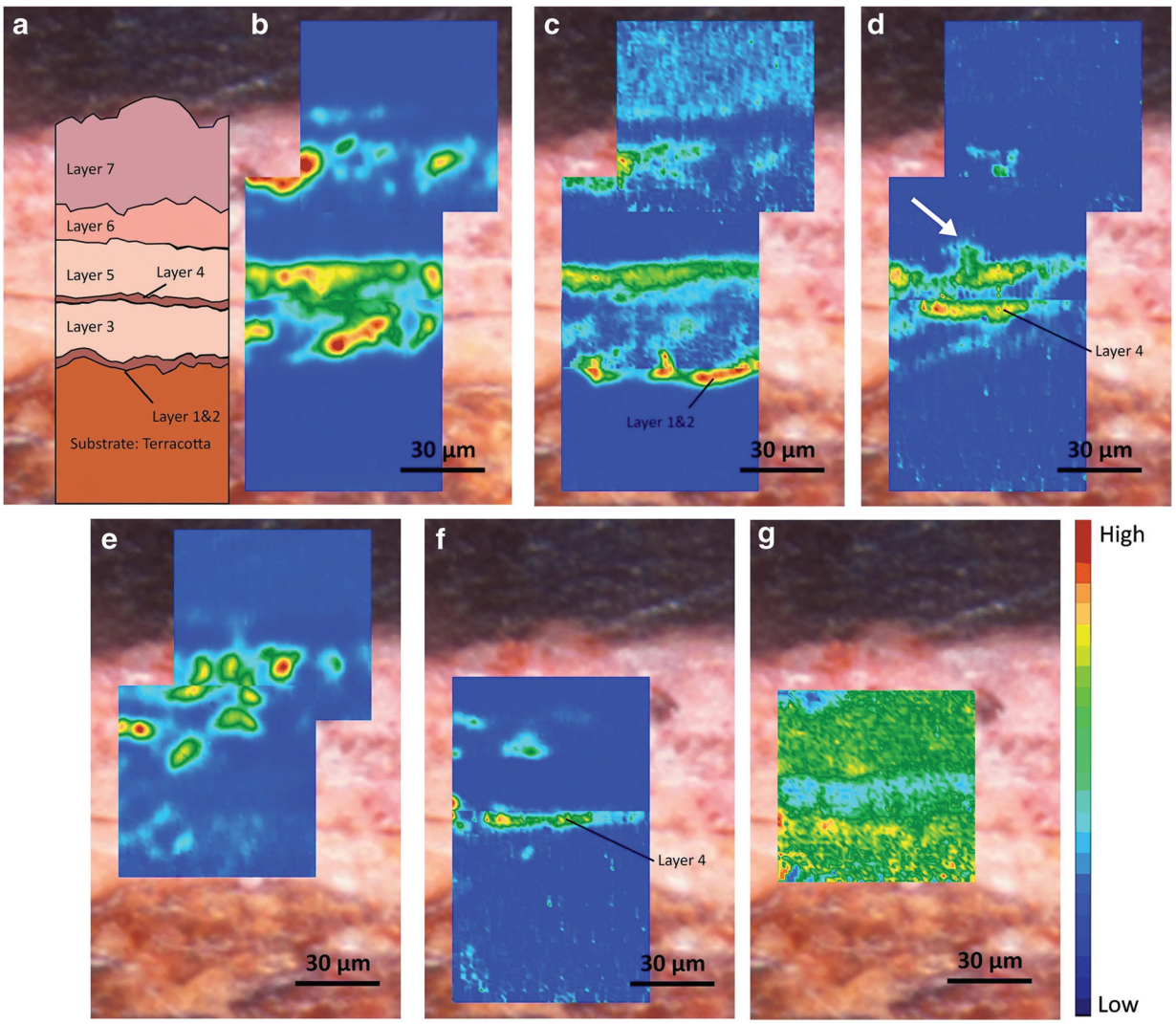

Fig. 4 (a) Optical microscopic image of the cross section from the 7-layer painted materials on the terracotta statue. Chemical images displaying the distribution of (b) lead white, (c) lipid—siccative oil, (d) lead carboxylates, (e) gypsum, (f) protein, and (g) calcium oxalates. Reprinted with permission,[94] copyright (2020) Springer Nature.

calcium carbonate ($CaCO_3$), *etc*.[108,109] The chemical compositions of paper vary depending on manufacture approach. Knowledge of chemical compositions can contribute to authentication and discovering provenance of ancient paper heritage. However, paper materials typically constitute a wide variety of components, which might be difficult to be distinguished based solely on IR spectra. For example, absorbance at 1732 cm^{-1} could indicate the presence of hemicelluloses,[110,111] but this absorbance might result from oxidation of lignin,[112] which is also a deterioration phenomenon. Therefore, it is necessary to combine other scientific analytical equipment to obtain comprehensive characterisation of paper heritage.

3.2.2 Case studies. Originating in China, paper has been developed and utilised as the main material for recording words or information for many centuries.[113] Properties of paper have altered and varied region by region as the technology of paper production transferred from China through Central Asia to the West. In Europe, the manufacture of paper has evolved, and compositions of paper include cellulose, wood pulp, sizing agents, fillers and coatings. A research study[114] investigating paper heritage from 12th century to date using ATR-FTIR spectroscopy discovered that between 1100–1300 A.D., paper was made up of rag sized with starch, while between 1400–1700 A.D., paper was composed of rag sized with gelatine. In the 1800–1960 (*ca.*) A.D. samples, wood pulp was characterised by the lignin absorption bands. This finding is crucial because the use of wood pulp as raw materials would lead to rapid deterioration of paper.[115] Modern paper (1960–today A.D.) utilised $CaCO_3$ as fillers to stabilise acid reaction. The presence of $CaCO_3$ can be detected with ATR-FTIR spectroscopy.[114,115] If large quantities of $CaCO_3$ are used in manufacture of paper, it can affect the mechanical properties of paper.

Islamic paper, manufactured in Islamic cultural areas including the Arab, Persian or Turkic realm, is distinct from other regions due

Table 2 Compounds detected in Fig. 4 with their integrated bands, vibration mode and peak wavenumbers. ν_{as} and ν_{sy} stand for antisymmetric and symmetric stretching modes, respectively. Reprinted with permission,[94] copyright (2021) Springer

Compounds	Integrated bands (cm^{-1})	Vibration mode	Peak wavenumber (cm^{-1})
Lead white—basic lead carbonate (synthetic analogue of hydrocerussite, $2PbCO_3{\cdot}Pb(OH)_2$)	1482–1288	$\nu_{as}(CO_3^{2-})$	~1392–1384
Lead white—lead carbonate (synthetic analogue of cerussite, $PbCO_3$)	1482–1288	$\nu_{as}(CO_3^{2-})$	1365
Lead carboxylates	1558–1480	$\nu_{as}(COO^-)$	1515
Lipid—siccative oil	1780–1692	ν_{sy}(C═O ester)	1738
Gypsum	1163–1056	$\nu_{as}(SO_4^{2-})$	1111
Protein	1667–1592	ν(C═O amide I)	1638
Calcium oxalates	1327–1310	ν_{as}(CO)	1320

to its unique papermaking process.[116] Fig. 6a displays two pieces of Islamic paper at UCL Institute for Sustainable Heritage.[117] In ATR-FTIR spectra for the Islamic paper, proteinaceous coatings such as casein or egg white can be detected by detecting the peaks of amide group bonds at 1533 and 1639 cm^{-1}, as shown in Fig. 6b.

Papermaking approaches travelled from the Arabic countries to Italy,[118] and it is in Italy that a technological evolution occurred leading to creation of a new kind of paper. This new kind of paper replaced the previous kind which originated from China and earned a name of "the manufactured western paper".[119] A research study analysed a series of Italian paper samples from Fabriano and Camerino which were produced between 13th–15th century,[119] as shown in Fig. 6c. In both areas, starch (which has the peak at 998 cm^{-1}) was not detected and possible use of animal gelatine (which has the peptide bond at 1540 and 1645 cm^{-1}) was proposed based on ATR-FTIR spectra results. Restoration using Tylose, a cellulose ether, might have caused the gelatine peaks less obviously, as shown in Fig. 6d. Furthermore, ATR-FTIR spectroscopy successfully identified the presence of $CaCO_3$, the alkali carbonate added in the manufacture of modern paper by looking at the characteristic bands at around 1410–1430 cm^{-1}. This finding can explain the historiographical conclusion that Fabriano was the centre of promoting the technological revolution which spread in Italy in 13th century and later throughout Europe.

Back to China, the birthplace of papermaking, technology of paper manufacture has been refined and a wide variety of paper artefacts could be seen in the history of traditional handmade paper.[120] *La Jian*, invented in Sui-Tang period (6th–10th centuries) and massively produced in Qing dynasty (17th–20th centuries), is famous for its aesthetic decoration with gold or silver flecks,[121] as shown in Fig. 6e. In a study *La Jian* was investigated with ATR-FTIR spectroscopy and it was discovered that the dyed surface was coated with Chinese insect

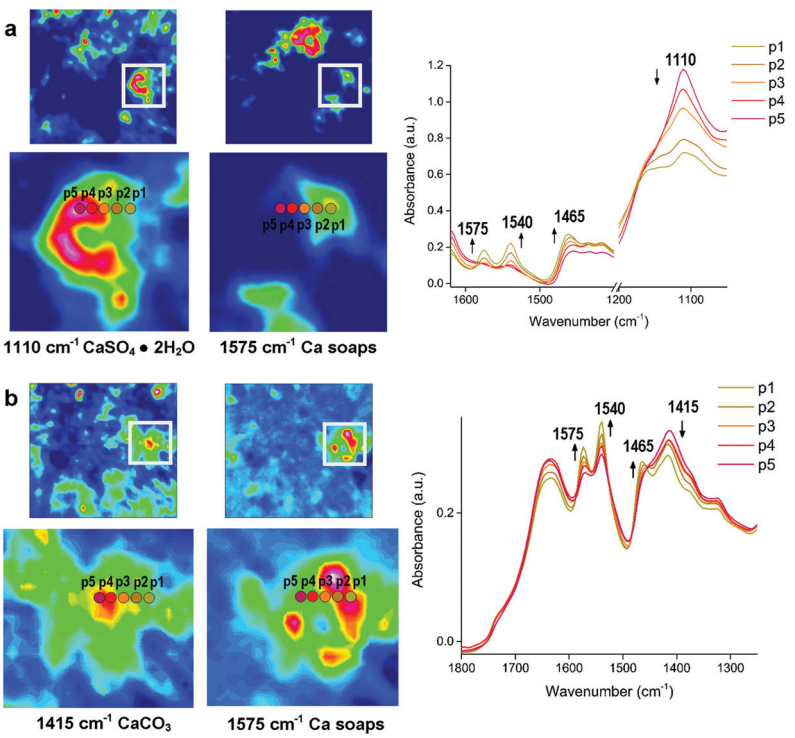

Fig. 5 ATR-FTIR spectroscopic imaging of the samples from surface of two leather books: (a) 17th century manuscript, showing the distribution of gypsum (1110 cm^{-1}) and Ca stearate (1575 cm^{-1}) and (b) the manuscript dated 1750, showing the distribution of $CaCO_3$ (1415 cm^{-1}) and Ca stearate. p1 to p5 represent pixel 1 to 5 where FTIR spectra are extracted. The chemical images of the integrated absorbance and the locations (p1 to p5) show the increasing absorbance of the Ca stearate as decreasing absorbance of the carbonate and sulphate. Reprinted with permission,[95] copyright (2018) American Chemical Society.

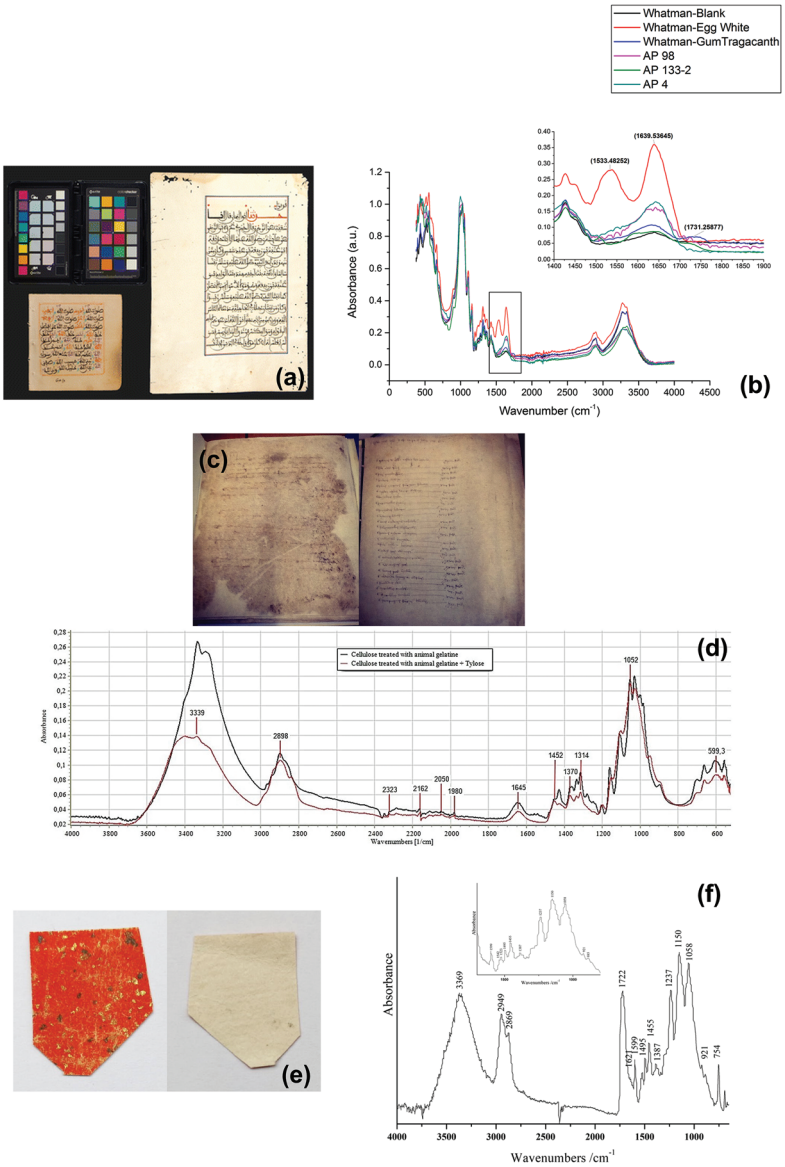

Fig. 6 (a) Two objects in the historic reference material collection at UCL Institute for Sustainable Heritage and (b) the proteinaceous coatings have peaks of amide group bonds at 1533 and 1639 cm^{-1} in ATR-FTIR spectra. Reproduced with permission,[117] copyright (2016) Springer Nature. (c) Paper documents from Camerino. (d) ATR-FTIR spectra of cellulose samples show that the restoration materials Tylose may make gelatine spectral bands at 1540 and 1645 cm^{-1} less visible. Reproduced with permission,[119] copyright (2020) Elsevier Masson SAS. (e) Lajian paper sample with Au/Ag flakes and upper orange-red layer (left) and backing layer (right), coated with (f) Chinese insect wax which has absorbance of carboxyl group at 1722 cm^{-1}. Reproduced with permission,[121] copyright (2019) Springer Nature.

wax[121] which has carboxyl group band at 1722 cm^{-1}, as shown in Fig. 6f. *Fen Jian*, another example of Chinese paper artefact that was commonly used in calligraphy, was examined in a project,[122] as shown in Fig. 7a. Chemical distribution and spectra of pigments (lead white: 1415, 1046, 681 cm^{-1}), paper fibre (cellulose: 1036, 1060, 1111, 1162 cm^{-1}) and ground ash (talc: 3674 cm^{-1}, lime: 1405, 876 cm^{-1}, and clay minerals: 1021 cm^{-1}, Si–O anti-symmetric stretching vibration) were confirmed using the ATR-FTIR mapping approach, as displayed in Fig. 7b and c.

ATR-FTIR spectroscopy has also been applied to investigate other paper-based cultural heritage such as photographs[123] and stamps.[124]

3.3 Textile

3.3.1 FTIR spectra of synthetic and natural fibres. A variety of measurement methods can be adopted to investigate fibres of textiles. If a fibre is not too thick, it may be examined with transmission measurement. However, when investigating a thick fibre, reflection modes especially ATR may be more useful. IR spectra databases for fibres have been established to identify unknown fibers.[125,126] The IR spectra databases can contribute to forensic analysis for fibres including the approximate dating and manufacturing process of textiles.[127]

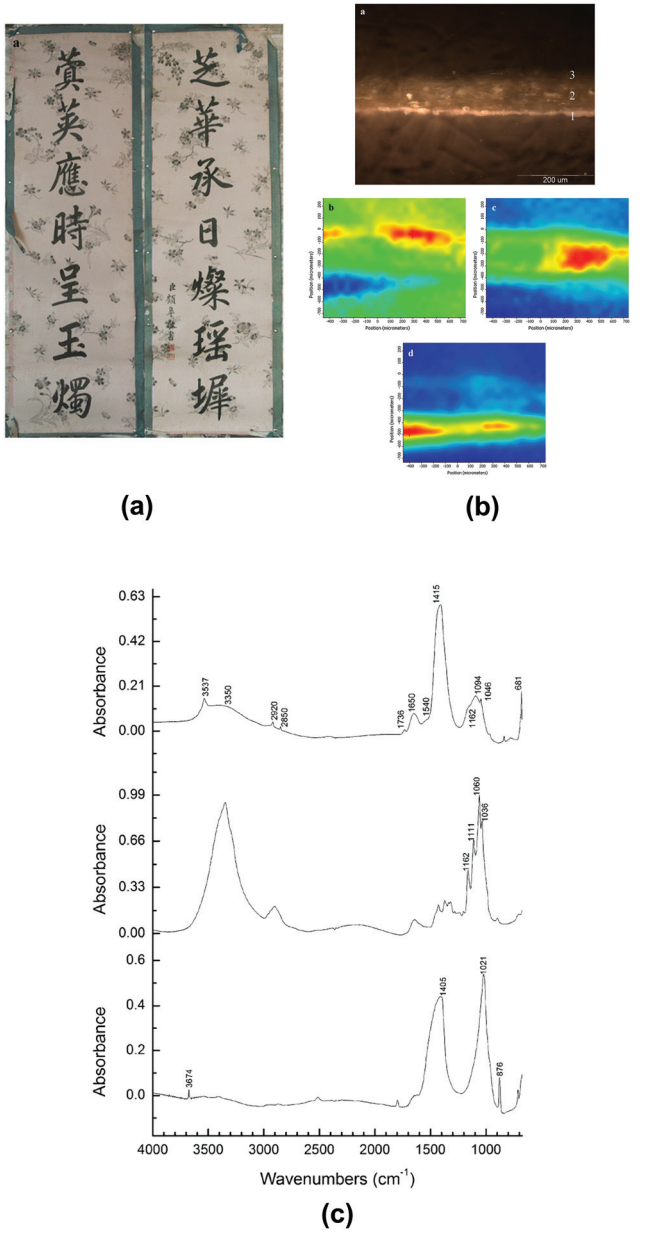

Fig. 7 (a) The piece of calligraphy *Tie Luo* (132.5 cm × 42 cm, which uses the *Fen Jian* with coloured pigment coating. (b) Micrograph (top) and ATR-FTIR mapping of cross-section of *Tie Luo* shows chemical distributions of pigment layer (middle left), paper fibre (middle right) and ground ash (bottom). (c) ATR-FTIR spectra of different locations in pigment layer (top), paper fibre layer (middle) and ground ash layer (bottom). Reproduced with permission,[122] copyright (2018) Springer Nature.

Synthetic fibres such as acrylics, nylons and polyesters, which are manufactured from polymers and copolymers of varying composition, can be distinguished using FTIR spectroscopy. Taking nylon as an example, nylon 6 and nylon 12 can be distinguished by comparing their IR spectra. In the two spectra, the important differences reside in the relative intensities of the band in the region 3000–2800 cm^{-1} (C–H stretching) and the position of the amide II band (N–H bending and C–N stretching).[128,129]

The main constituents of natural textile fibres such as cotton, silk, wool, hemp and flax are proteins, leading to an apparently similar spectral pattern. However, FTIR spectroscopy is also useful for identification of natural textile fibres by comparing different types of proteins these fibres possess. For example, silk is made of fibroin, whereas wool is composed of keratin. The different composition of these proteins results in different intensities of bands in IR spectra of wool and silk.[130]

3.3.2 Case studies. There are plenty of methods for identification of textile fibres including the SEM method, dissolution methods and combustion methods.[127] However, SEM results can only provide microstructure information but lack molecular information; combustion methods sacrifice a portion of test textile samples. ATR-FTIR spectroscopy has been utilised as a useful tool which may need no or micro sample preparation to characterise fibre types of textiles. Plant and animal are basically the two types of textile fibres. Flax fibre was identified as the main material of historical textiles from the Imperial Pavilion (Hunkar Kasri),[131] as shown in Fig. 8a. In the ATR-FTIR spectra from Imperial Pavilion samples typical bands of flax could be observed (*e.g.*, the 1029 cm^{-1} and 1104 cm^{-1} bands attributed from CO stretching of primary and secondary alcohol), as shown in Fig. 8b.[131] Silk fibre was characterised from sutras[132] and theatrical figurines[133] excavated in China, as shown in Fig. 8c, with typical absorption bands at 1636 cm^{-1} (C=O stretching vibrations in amide I) and 1525/1510 cm^{-1} (N–H bending vibrations in amide II), as shown in Fig. 8d. Apart from fibre structure, pigments and dyes on textile can also be identified using ATR-FTIR spectroscopy.[131–134]

A study by Raditoiu *et al.* analysed a traditional pillowcase from Moldova,[135] as shown in Fig. 8e. The historical pillowcase, manufactured in 19th–20th centuries, consists of two parts: the support textile fibre and the coloured fibre. ATR-FTIR spectra support the belief that textile fibre is flax, while the coloured fibre is wool fibres. It is easier for wool to be identified using ATR-FTIR due to the characteristic bands of amide I, amide II and other intense bands such as 1390 cm^{-1} (CH_3 symmetrical deformation) and 1055 cm^{-1} (antisymmetric stretch C–O–C and C–N stretch), as shown in Fig. 8f. However, distinguishing flax and hemp would be difficult because of their similarities in the spectra. Raditoiu *et al.* adopted an absorbance ratio method where I_{1595}/I_{1105} and I_{1595}/I_{2900} were calculated. Values of I represent band intensities. Flax and hemp have different I_{1595}/I_{1105} and I_{1595}/I_{2900} calculated from the spectra and thus this can contribute to differentiation of the two types of fibres.

3.4 Polymers

3.4.1 FTIR spectra of polymers. Plastics, polymeric materials, or synthetic polymers are common in cultural heritage nowadays. Some polymers such as acrylics, alkyds and polyvinyl acetate (PVA) have been used considerably in modern paint binders[136] in addition to the natural binders discussed in Section 3.1.1. Since the 1870s when John Wesley Hyatt synthesised the first commercial plastic—celluloid, polymeric

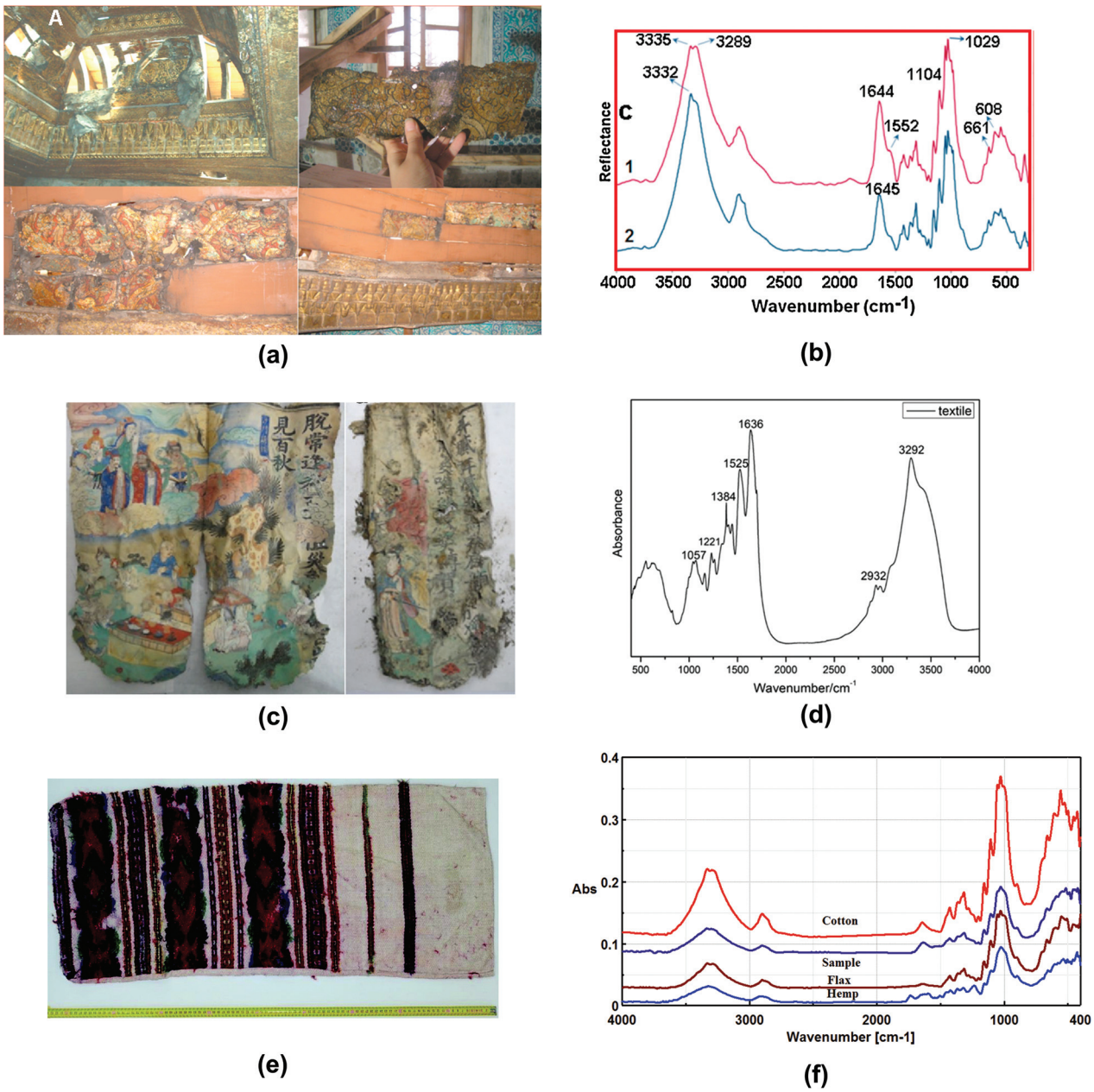

Fig. 8 (a) The photographs of the ceiling of the audience room (top right), before restoration, where one of the samples was taken (top left) and the lower part of the ceiling (bottom left), where the other sample was taken (bottom right). (b) ATR-FTIR spectra of Imperial Pavilion samples shows typical bands of flax at 1029 cm^{-1} and 1104 cm^{-1}. Reproduced with permission,[131] copyright (2017) Elsevier Masson SAS. (c) Pages of the sutra and (d) ATR-FTIR spectra of the sutra shows characteristic bands at 1636 cm^{-1} (amide I) and 1525/1510 cm^{-1} (amide II). Reproduced with permission,[132] copyright (2019) Springer Nature. (e) Traditional pillowcase originating from Moldavia historical region, manufactured at the end of the 19th century to beginning of the 20th century. (f) ATR-FTIR spectra of the sample of traditional pillowcase and other fibres. Reproduced with permission,[135] copyright (2019) Springer Nature.

materials have contributed to industrial, social and cultural progress. An increasing number of synthetic polymers were used to mimic more luxurious materials such as tortoiseshell and ivory[137–139] because of the artistic interpretation these synthetic polymers could offer. In a survey conducted at the British Museum in 1990s, the number of polymer objects was more than 3000.[140] The kinds of these polymer objects included cellulose acetate (CA), cellulose nitrate (CN), Bakelite (phenol formaldehyde), polyethylene, polypropylene, polyurethane, polystyrene, polyvinyl chloride (PVC), nylon and rubber. FTIR spectroscopy is one of the most common techniques used to investigate these polymers in cultural heritage.[141–143]

Some polymer-based cultural heritage may produce degradation products that can cause harm to other heritage, such as CA, CN and PVC which emit acetic acid, nitric acid or hydro-

chloric acids, respectively, to the environment during the process of degrading.[144–147] An example of plastic heritage that may produce harmful components is cinematographic and photographic films.[148,149] Both films are made of CA and CN which are physically similar. FTIR spectroscopy can assist in distinguishing CA and CN as a result of their different spectra. The nitrate shows a strong band near 1650 cm^{-1} due to nitrogen dioxide (NO_2) stretching, while the acetate shows a strong band near 1730 cm^{-1} attributed to C=O stretching. Their spectral patterns vary as their conditions deteriorate, by detecting increasing absorbance of CN at 1730 cm^{-1} (carbonyl region) and decreasing absorbance at 1650 cm^{-1} (nitro groups).[150]

In addition to the polymeric cultural heritage objects mentioned above, plastics can also be applied to restoration work for cultural heritage. Restoration materials such as adhesives, coatings, fixatives and consolidants can be added onto cultural heritage objects for supporting, storing and packaging. Curators and conservators may need to monitor these restoration materials because these materials may interact with the cultural heritage objects, adversely affecting physical or chemical properties of the objects. Therefore, identification of restoration materials is of importance for ensuring long-term use, exhibition and storage of cultural heritage objects. Bell *et al.* has analysed 15 common plastics that can be observed in museum collections using ATR-FTIR and ER-FTIR spectroscopies.[151] A comparative spectral study of these plastics and a flowchart method for examining plastic objects in museums are provided in the research of Bell.

3.4.2 Case studies. The majority of ATR-FTIR polymer applications focus on measurement of chemical compositions and deterioration. There is great diversity of synthetic polymers used in cultural heritage. Research examining 12 audiotapes produced during 1950–1980 discovered that different types of polymers involving PVA, CA, PET, cellulose acetate phthalate (CAP) and polyester urethane (PEU) comprised either magnetic or non-magnetic sides of the tapes.[152] The main deterioration of magnetic tapes is hydrolysis which would lead to break down of the tapes. The name of the consequence of hydrolysis of the tapes is sticky shed syndrome (SSS) or soft binder syndrome (SBS).[153,154] SSS and SBS are normally referred to as the same degradation which stickiness, shedding, and squealing can be observed on the tapes, while SSS is used exclusively when the syndrome is caused by exposure to heat. SSS/SBS can be detected and measured using ATR-FTIR spectroscopy.[152,153] In ATR-FTIR spectra, SSS/SBS tapes display free carbonyl bands at 1724 cm^{-1} with a shoulder at 1701 cm^{-1}, while non-SSS/SBS tapes show the most intense bands at 1698 cm^{-1}.

Photographic and cinematographic films, video recordings with cultural and historical value, have received significant attention since the end of 20th century due to their composition of CN and CA. As mentioned in Section 3.4.1, these two types of polymers would release harmful acids that might adversely affect the environment leading to further deterioration. As a result, to monitor conditions of CN/CA based cultural heritage and establish early warning systems are of great importance. Degree of substitution (DS) has been utilised to describe the state of the state of conservation of historical films.[155] DS of a polymer is the average number of substituent groups attached per base unit or monomeric unit.[156] In research of historical films,[155] DS was calculated based on ATR-FTIR spectra. In the ATR-FTIR spectra, bands at 3330 cm^{-1} (OH stretching) and 1030 cm^{-1} (COC stretching) were chosen to determine DS value for CA, as shown in Fig. 9a, while bands at 1636 cm^{-1} (nitrate antisymmetric stretching) and 1060 cm^{-1} (COC stretching) were selected to determine DS for CN, as shown in Fig. 9b. The DS values obtained with ATR-FTIR spectroscopic measurements suggested that a sample of CA historical reel was in the poor conservation condition with lower values ranging from 1.36 to 0.76, as displayed in Fig. 9c, compared to other samples of cinematographic films with higher values ranging from 1.76 to 1.93 (not shown here). The results were in agreement of the significant deterioration where a strong vinegar odour emitted from the historical reel was observed. DS values of this CA historical reel also indicated that the inner parts of the reel were in more severe state of deterioration where CA was covered from both sides because of film winding. The initial (original) DS of CN and CA obtained with ATR-FTIR spectroscopy used in this research were 2.26 and 2.3–2.4, respectivley.[155,157]

Artificial and accelerated ageing is a treatment for investigating degradation of research samples[158] in a shorter time period compared to natural degradation. The objective of artificial accelerated aging is to speed up the changes in the properties of samples because natural ageing is often a slow process that would take several or even a hundred years.[159] This artificial accelerated ageing is a significant treatment to study plastic cultural objects because it may contribute to understanding of the degradation mechanism and extend the lifetime of plastic cultural heritage. Thermal or photochemical degradation is commonly explored with regards to plastics. PVC[160] and celluloid (CN mixed with Camphor)[150] materials that can be found in museum collections have been investigated using ATR-FTIR spectroscopy for their thermal and photo degradation under elevated temperature and light irradiation. These studies explore ATR-FTIR spectroscopic technique as a potential tool to monitor the degradation of plastic objects from museum collections and provide insights for conservation strategies.

3.5 Inorganic substances: stone, ceramics and glasses

Although FTIR spectroscopy is especially useful for studying organic and complex samples, there has been an increasing amount of research that utilises FTIR spectroscopy to investigate inorganic objects, such as stone,[161–163] ceramics[164–169] and glasses.[170–172] due to the well-established and comprehensive IR databases of minerals.[173–176] Minerals are the main ingredient to produce ceramics and glasses. The dissimilarity between ceramics and glasses is that ceramics are crystalline, while glasses are amorphous. The mineral com-

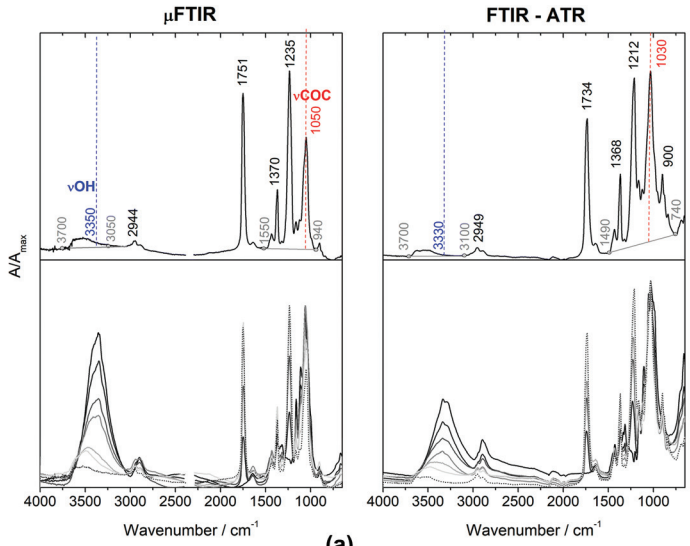

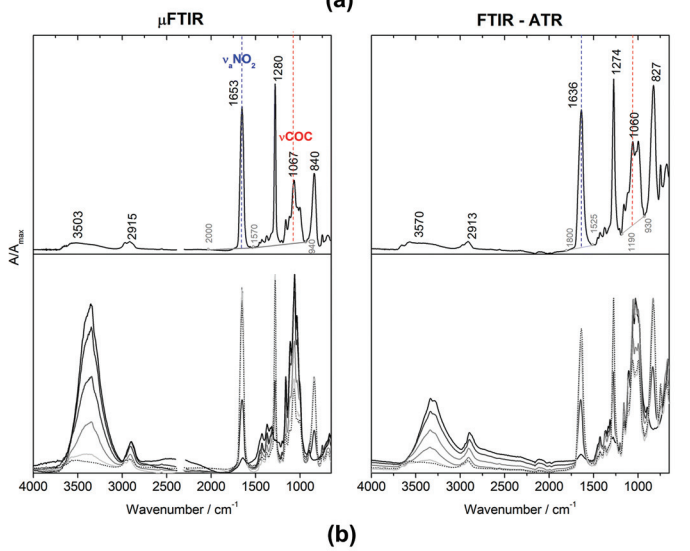

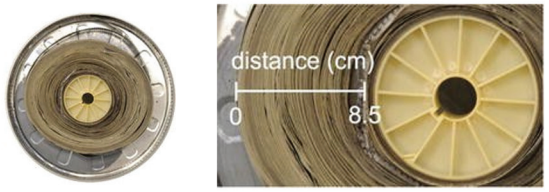

Distance (cm)	0	0.9	1.8	2.7	3.5	5	5.5	5.8	6.8	8.5
DS by μFTIR	1.39	1.01	1.02	0.87	0.83	0.88	0.85	0.85	0.83	0.84
DS by ATR	1.36	0.79	0.76	0.82	0.80	0.78	0.83	0.83	0.79	0.78

(c)

Fig. 9 Micro FITR (μ-FTIR) in transmission mode and ATR-FTIR spectra of (a) CA and (b) CN, where 3330, 1030 cm^{-1} and 1636, 1060 cm^{-1} are used to produce DS values. (c) DS values of CA of a historical reef from the inner parts to outer parts acquired using μ-FTIR and ATR-FTIR. Reproduced with permission,[155] copyright (2020) Springer Nature.

pounds for manufacturing ceramics are generally oxides, nitrides, carbides and borides. These mineral compounds have their characteristic IR bands and therefore can be identified with FTIR spectroscopy.[177,178] Glasses have wide composition ranges; however, the main contents are generally silicate-based materials. Glasses may experience structural changes resulting from the leaching of alkaline and earth alkaline glass compounds. The structural changes cause shifts of wavenumber and changes of intensities to the non-bridging and bridging Si–O stretching bands at 950 cm^{-1} and 1050 cm^{-1}, which can be detected with FTIR spectroscopy.[170]

Stone heritage may be likely to suffer from changes in environmental conditions including the presence of water, air pollutants and biodegradation. Deposits on the surface of stone heritage attributed from environmental impacts can be effectively diagnosed using the FTIR techniques.[179,180] Limestone and marble ($CaCO_3$), worldwide used for stone heritage as well as historical architecture, have been suffered from degradation due to air pollutants in urban areas.[161–163] In ATR-FTIR spectra, bands at around 1405, 872 and 712 cm^{-1} are typical vibrations of $CaCO_3$,[58] corresponding respectively to antisymmetric C–O stretch, C–O out-of-plane bend and C–O in-plane bend in CO_3^{2-}. The degradation products can be detected using ATR-FTIR spectroscopy[161,162] including gypsum ($CaSO_4{\cdot}2H_2O$) due to due to SO_2 attack and oxalate ($CaC_2O_4{\cdot}nH_2O$) due to biological weathering. Typical bands assigned to identify these degradation products are at 1110 cm^{-1} (antisymmetric stretch vibration mode of SO_2) for gypsum and at 1618 and 1321 cm^{-1} (antisymmetric and symmetric CO_2 stretching modes, respectively) for calcium based oxalate.[161] In a very recent study of the Carrara marble and its treatment was studied *in situ via* ATR-FTIR spectroscopy and with macro ATR-FTIR spectroscopic imaging.[181]

In the case of ceramics, FTIR spectroscopy is able to identify mineralogical compositions,[168] firing temperature and atmosphere.[169] ATR-FTIR spectroscopy combined with principal component analysis (PCA) has been utilised to classify Hellenistic and Roman ceramic shards and determine their firing temperature.[182] XRD is the most commonly used technique to conduct qualitative and quantitative analysis of mineralogical sample.[183] ATR-FTIR spectroscopy combined with partial least squares (PLS) regression method has been utilised as an alternative technique to XRD to quantify 7 groups of minerals in archaeological and cultural heritage samples containing clay material.[184] Compared to a rather large amount of sample required for XRD measurements (~0.5–1 g), smaller amount (~a few mg) is needed for ATR-FTIR spectroscopic measurements, one of the advantages for investigating cultural heritage when considering minimizing the loss of the cultural heritage objects. In the case of glasses, ATR-FTIR spectroscopy can be employed to detect the degree of degradation.[172] 19th century daguerreotypes have been investigated their glass degradation using ATR-FTIR spectroscopy.[171] These studies and applications demonstrate that ATR-FTIR spectroscopic technique is a potential and useful tool for the analysis of cultural heritage objects composed of inorganic materials.

4. Future outlook for ATR-FTIR spectroscopy and imaging for cultural heritage applications

It is hoped that this review has highlighted the use of ATR-FTIR spectroscopy and spectroscopic imaging for investigation of cultural heritage. Although ATR-FTIR spectroscopy and spectroscopic imaging techniques are widely used as powerful analysis tools for cultural heritage, there is still some potential for more advanced development. It is well-known that the depth of penetration of the evanescent wave into the investigated sample can be adjusted by varying the angle of incidence using apertures.[185] As a result, a depth profiling analysis of the sample can be performed by collecting IR spectra into the sample at different depths. The depth profiling analysis has been conducted for identification of multilayer polymer laminates using macro[186] and micro[26] ATR-FTIR spectroscopic imaging.

Depth profiling of objects of cultural heritage has been pioneered in the author's laboratory.[187] Fig. 10 shows the depth profiling using micro ATR-FTIR spectroscopic imaging of the surface of a jewellery box dated 1920 from the V&A museum study collection.[187] The jewellery box was a degrading CN

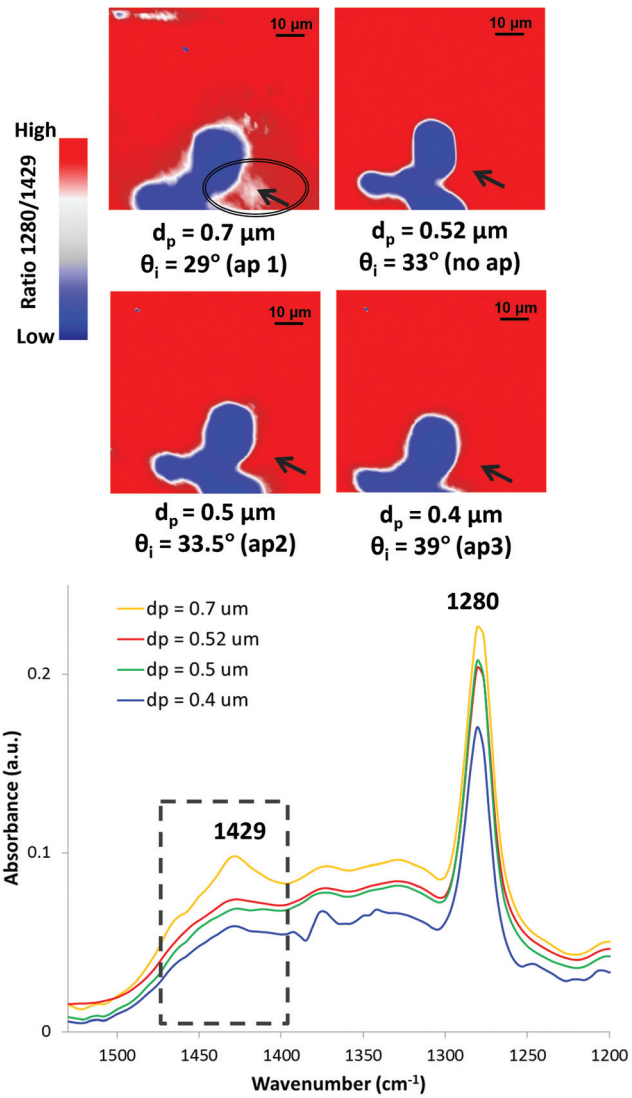

Fig. 10 Depth profiling of the surface of the CN jewellery box using micro ATR-FTIR spectroscopic imaging in the area corresponding to blistering. Reprinted with permission.[187]

object that might emit harmful components as discussed in Section 3.4. The ATR-FTIR spectra show increasing absorbance of CN at 1280 cm^{-1} (symmetric stretching of the NO_2 ester groups) as the depth of penetration increases (the angle of incidence decreases). By using the smaller angle of incidence (29°, aperture 1) which enables a deeper thickness to be probed, the band at 1429 cm^{-1} (δCOH) attributed to the alcohol species forming blisters beneath the surface of historical jewellery box can be detected. ATR-FTIR spectroscopy and imaging has been successfully and commonly applied to investigation of historical plastics due to its minimal to no sample preparation. It is expected that the method of depth profiling can make a valuable contribution to performing analysis of more samples and objects of cultural heritage in a non-destructive way.

Developments toward handheld or portable spectrometers allow ATR-FTIR spectroscopy to be employed in field-based or *in situ* research,[151,188,189] whilst most of cultural heritage research using ATR-FTIR spectroscopy is still lab-based. External Reflection (ER) and Diffuse Reflection (DR) modes have been used in portable FTIR devices to investigate cultural heritage[151,190,191] in excavation or storage sites, exempting artefacts from relocating frequently. One of the main advantages of ER and DR modes is that they are non-contact acquisition modes, allowing for completely non-invasive studies of cultural heritage materials. However, spectra in ER and DR modes may show distortions resulting from volume and surface reflection of light.[24] These distortions may lead to false spectral interpretation. Aside from spectral distortions, ER and DR can only detect shallow surfaces of examined objects.[191] Therefore, the spectra acquired in ER and DR modes may not be representative of the whole objects, especially when the objects show an inherent chemical heterogeneity. Although ATR mode requires contact between the crystal and the sample, it can reach higher lateral resolution in FTIR experiments compared to ER and DR modes.[9] It can be anticipated that with developments and advancements of improving the set up for optimising the required ATR crystal contact, ATR mode can advance toward more mobile and non-destructive measurement where results are representative of the cultural heritage sample.

As briefly mentioned in Section 3.2.1, the use of synchrotron radiation (SR) light sources can enhance spectral quality for FTIR studies. FTIR imaging using an FPA detector coupled with SR light sources for investigation of cultural heritage has been conducted in external reflection[86,192] and transmission modes.[192] There is paucity of research on investigation of cultural heritage utilising ATR-FTIR imaging coupled with SR. It is expected that more exploitation and development of ATR-FTIR imaging with the use of SR may be achieved for investigation of cultural heritage.

Although chemical components of cultural heritage may be complex and aged, leading to difficulties in analysing spectra, it is also a possibility for rapid identification of heritage materials by building comprehensive spectral libraries and databases. IRUG[193] provides database which strongly supports interpretation and identification of spectra. As mentioned in this review, spectral databases for various categories of cultural heritage materials have been built.[49,50,58–60,124,141,173–176] Nevertheless, spectra may be extremely complicated and thus difficult to be identified. To help analyse FTIR spectra, chemometric methods have been applied to assess variations between the spectra as discussed in this review.[6,92,93,108,114,182,189,194] The chemometric methods can categorise the samples and also cope with distorted spectra, contributing enormously to data analysis. It is hoped that the combination of spectral data bases, chemometrics and portable ATR-FTIR spectrometer[195] can be developed and commercialised. The development of these systems will mean that ATR-FTIR spectroscopy can be employed by investigators without professional spectral knowledge to examine cultural heritage and artifacts *in situ*.

5. Conclusions

FTIR spectroscopy is a well-established analytical technique that has been applied in the cultural heritage field for identification and characterisation of original materials, degradation and restoration/conservation products, and monitoring of cleaning treatments. ATR-FTIR spectroscopy and ATR-FTIR spectroscopic imaging are very suitable methods for investigation of cultural heritage materials due to its minimal requirements for sample preparation and its provision for high resolution. Moreover, ATR-FTIR spectroscopic instrumentation can be not only traditional single point detection, but also two-dimensional mapping and imaging, which is especially beneficial for multi-layered structure cultural objects such as painting, historical paper and polychrome sculptures. Applications of ATR-FTIR spectroscopy and spectroscopic imaging on cultural heritage have been explored and the findings are of significance to archaeology and conservation management of cultural heritage. However, there are still many opportunities for advanced utilisation of ATR-FTIR spectroscopy and spectroscopic imaging and some striking improvements for ATR-FTIR spectroscopy and spectroscopic imaging can be anticipated, such as depth profiling and *in situ* portable spectrometers, to investigate a wide variety of cultural heritage. This review has highlighted the use of ATR-FTIR spectroscopy and spectroscopic imaging for the study of cultural heritage. It is hoped that future research will facilitate these techniques in cultural heritage field and that ATR-FTIR spectroscopy and spectroscopic imaging will play an important role in archaeometry, archaeological science and conservation science.

Conflicts of interest

There are no conflicts to declare.

Acknowledgements

We thank our many colleagues and collaborators in the area of applications of ATR-FTIR spectroscopic imaging, including Marika Spring and David Peggie (The National Gallery, London), Alessandra Vichi (Swiss Institute of Art Research), Satoka Tanimoto (Imperial College London), Boris Pretzel, Brenda Keneghan and Lucia Burgio (V&A Museum, UK), Gayane Eliazyan (Matenadaran, Armenia), Elena Possenti (ISPC-CNR, Milan, Italy), Silvia Prati and Rocco Mazzeo (University of Bologna, Italy), Francesca Rosi and Costanza Miliani (CNR-ISTM, Italy) and our colleagues at the Institute for Molecular Science and Engineering (IMSE) and the Science and Engineering Research for Cultural Heritage Network at Imperial College London (**https://www.imperial.ac.uk/cultural-heritage-research/people/**).

References

1 M. S. Tite, *Archaeometry*, 1991, **33**, 139–151.
2 National Academy of Sciences, *Scientific Examination of Art: Modern Techniques in Conservation and Analysis*, The National Academies Press, Washington, DC, 2005.
3 G. Artioli and I. Angelini, *Scientific Methods and Cultural Heritage: An Introduction to the Application of Materials Science to Archaeometry and Conservation Science*, Oxford University Press, Oxford, 2010.
4 P. T. Craddock, *Scientific Investigation of Copies, Fakes and Forgeries*, Routledge, London, 2009.
5 K. Trentelman, *Annu. Rev. Anal. Chem.*, 2017, **10**, 247–270.
6 P. Peets, I. Leito, J. Pelt and S. Vahur, *Spectrochim. Acta, Part A*, 2017, **173**, 175–181.
7 M. R. Derrick, D. Stulik and J. M. Landry, *Infrared Spectroscopy in Conservation Science*, Getty Conservation Institute, Los Angeles, 2000.
8 R. Salzer and H. Siesler, *Infrared and Raman Spectroscopic Imaging*, Wiley-VCH, 2nd edn, 2014.
9 F. Rosi, L. Cartechini, D. Sali and C. Miliani, *Phys. Sci. Rev.*, 2019, **4**, 20180006.
10 P. R. Griffiths and J. A. d. Haseth, *Fourier transform infrared spectrometry*, John Wiley & Sons, New Jersey, 2nd edn, 2007.
11 M. Milosevic, *Internal Reflection and ATR Spectroscopy*, John Wiley & Sons, New Jersey, 2012.
12 L. A. Averett, P. R. Griffiths and K. Nishikida, *Anal. Chem.*, 2008, **80**, 3045–3049.
13 M. Miljković, B. Bird and M. Diem, *Analyst*, 2012, **137**, 3954–3964.
14 E. H. Korte and A. Röseler, *Anal. Bioanal. Chem.*, 2005, **382**, 1987–1992.
15 M. Fox, *Optical properties of solids*, Oxford University Press, London, 2010.
16 M. Milosevic and S. L. Berets, *Appl. Spectrosc. Rev.*, 2002, **37**, 347–364.
17 F. Casadio and L. Toniolo, *J. Cult. Heritage*, 2001, **2**, 71–78.
18 M. J. D. Low and N. S. Baer, *Stud. Conserv.*, 1977, **22**, 116–128.
19 E. Kendix, G. Moscardi, R. Mazzeo, P. Baraldi, S. Prati, E. Joseph and S. Capelli, *J. Raman Spectrosc.*, 2008, **39**, 1104–1112.
20 R. G. Messerschmidt and M. A. Harthcock, *Infrared Microspectroscopy: Theory and Applications*, Marcel Dekker Inc, New York, 1988.
21 K. L. A. Chan and S. G. Kazarian, *Appl. Spectrosc.*, 2003, **57**, 381–389.
22 E. Joseph, C. Ricci, S. G. Kazarian, R. Mazzeo, S. Prati and M. Ioele, *Vib. Spectrosc.*, 2010, **53**, 274–278.
23 R. Ploeger, O. Chiantore, D. Scalarone and T. Poli, *Appl. Spectrosc.*, 2011, **65**, 429–435.
24 C. Miliani, F. Rosi, A. Daveri and B. G. Brunetti, *Appl. Phys. A*, 2012, **106**, 295–307.
25 K. L. A. Chan, F. H. Tay, G. Poulter and S. G. Kazarian, *Appl. Spectrosc.*, 2008, **62**, 1102–1107.
26 T. P. Wrobel, A. Vichi, M. Baranska and S. G. Kazarian, *Appl. Spectrosc.*, 2015, **69**, 1170–1174.
27 S. G. Kazarian and K. L. A. Chan, *Analyst*, 2013, **138**, 1940–1951.
28 K. L. A. Chan and S. G. Kazarian, *Chem. Soc. Rev.*, 2016, **45**, 1850–1864.
29 S. G. Kazarian and K. L. A. Chan, *Appl. Spectrosc.*, 2010, **64**, 135A–152A.
30 G. Steiner and E. Koch, *Anal. Bioanal. Chem.*, 2009, **394**, 671–678.
31 A. V. Ewing and S. G. Kazarian, *Analyst*, 2017, **142**, 257–272.
32 C. Ricci, K. L. A. Chan and S. G. Kazarian, *Appl. Spectrosc.*, 2006, **60**, 1013–1021.
33 C. L. Song and S. G. Kazarian, *Analyst*, 2019, **144**, 2954–2964.
34 Y. Hikima, J. Morikawa and S. G. Kazarian, *Anal. Chim. Acta*, 2019, **1065**, 79–89.
35 A. V. Ewing and S. G. Kazarian, *Spectrochim. Acta, Part A*, 2018, **197**, 10–29.
36 M. J. Bailey, N. J. Bright, R. S. Croxton, S. Francese, L. S. Ferguson, S. Hinder, S. Jickells, B. J. Jones, B. N. Jones, S. G. Kazarian, J. J. Ojeda, R. P. Webb, R. Wolstenholme and S. Bleay, *Anal. Chem.*, 2012, **84**, 8514–8523.
37 J. van Der Weerd, H. Brammer, J. J. Boon and R. M. A. Heeren, *Appl. Spectrosc.*, 2002, **56**, 275–283.
38 J. van der Weerd, R. M. A. Heeren and J. J. Boon, *Stud. Conserv.*, 2004, **49**, 193–210.
39 S. Prati, F. Rosi, G. Sciutto, P. Oliveri, E. Catelli, C. Miliani and R. Mazzeo, *Microchem. J.*, 2013, **110**, 314–319.
40 S. Prati, F. Rosi, G. Sciutto, R. Mazzeo, D. Magrini, S. Sotiropoulou and M. Van Bos, *Microchem. J.*, 2012, **103**, 79–89.
41 E. Pouyet, A. Lluveras-Tenorio, A. Nevin, D. Saviello, F. Sette and M. Cotte, *Anal. Chim. Acta*, 2014, **822**, 51–59.
42 C. Martin de Fonjaudran, A. Nevin, F. Pique and S. Cather, *Anal. Bioanal. Chem.*, 2008, **392**, 77–86.

43 Z. E. Papliaka, L. Vaccari, F. Zanini and S. Sotiropoulou, *Anal. Bioanal. Chem.*, 2015, **407**, 5393–5403.
44 M. Bacci, in *Modern Analytical Methods in Art and Archaeology*, Wiley-Interscience, ed. E. Ciliberto and G. Spoto, John Wiley & Sons Inc, New York, 2000, pp. 321–361.
45 C. Genestar and C. Pons, *Anal. Bioanal. Chem.*, 2005, **382**, 269–274.
46 S. Kuckova, I. Nemec, R. Hynek, J. Hradilova and T. Grygar, *Anal. Bioanal. Chem.*, 2005, **382**, 275–282.
47 S. Prati, E. Joseph, G. Sciutto and R. Mazzeo, *Acc. Chem. Res.*, 2010, **43**, 792–801.
48 E. Pięta, J. Olszewska-Świetlik, C. Paluszkiewicz, A. Zając and W. M. Kwiatek, *Vib. Spectrosc.*, 2019, **103**, 102928.
49 K. Castro, M. Pérez, M. Dolores Rodríguez-Laso and J. M. Madariaga, *Anal. Chem.*, 2003, **75**, 215a–221a.
50 R. J. Gettens, H. KÜHn and W. T. Chase, *Stud. Conserv.*, 1967, **12**, 125–139.
51 R. Ion, A. Nuta, A. Sorescu and L. Iancu, in *Photochemistry and Photophysics – Fundamentals to Applications*, ed. S. Saha and S. Mondal, IntechOpen, London, 2018, pp. 161–178.
52 S. Prati, M. Milosevic, G. Sciutto, I. Bonacini, S. G. Kazarian and R. Mazzeo, *Anal. Chim. Acta*, 2016, **941**, 67–79.
53 G. Sciutto, S. Prati, I. Bonacini, L. Litti, M. Meneghetti and R. Mazzeo, *Anal. Chim. Acta*, 2017, **991**, 104–112.
54 D. Quintero Balbas, S. Prati, G. Sciutto, E. Catelli and R. Mazzeo, *New J. Chem.*, 2019, **43**, 9411–9419.
55 M. Ortega-Avilés, P. Vandenabeele, D. Tenorio, G. Murillo, M. Jiménez-Reyes and N. Gutiérrez, *Anal. Chim. Acta*, 2005, **550**, 164–172.
56 E. Platania, N. L. W. Streeton, A. Lluveras-Tenorio, A. Vila, D. Buti, F. Caruso, H. Kutzke, A. Karlsson, M. P. Colombini and E. Uggerud, *Microchem. J.*, 2020, **156**, 104811.
57 A. Andreotti, I. Bonaduce, M. P. Colombini, G. Gautier, F. Modugno and E. Ribechini, *Anal. Chem.*, 2006, **78**, 4490–4500.
58 S. Vahur, A. Teearu, P. Peets, L. Joosu and I. Leito, *Anal. Bioanal. Chem.*, 2016, **408**, 3373–3379.
59 S. Vahur, U. Knuutinen and I. Leito, *Spectrochim. Acta, Part A*, 2009, **73**, 764–771.
60 S. Vahur, A. Teearu and I. Leito, *Spectrochim. Acta, Part A*, 2010, **75**, 1061–1072.
61 C. Cucci, J. K. Delaney and M. Picollo, *Acc. Chem. Res.*, 2016, **49**, 2070–2079.
62 J. K. Delaney, M. Thoury, J. G. Zeibel, P. Ricciardi, K. M. Morales and K. A. Dooley, *Heritage Sci.*, 2016, **4**, 6.
63 M. Corradini, L. de Ferri and G. Pojana, *Appl. Spectrosc.*, 2020, **75**, 445–461.
64 M. Corradini, L. de Ferri and G. Pojana, *J. Raman Spectrosc.*, 2021, **52**, 35–58.
65 T. Ford, M. Iwanicka, E. Platania, P. Targowski and E. Hendriks, *Eur. Phys. J. Plus*, 2021, **136**, 899.
66 V. Di Tullio and N. Proietti, *Magnetochemistry*, 2020, **6**, 21.
67 A. Doria, G. P. Gallerano, E. Giovenale, L. Senni, M. Greco, M. Picollo, C. Cucci, K. Fukunaga and A. C. More, *Appl. Sci.*, 2020, **10**, 7661.
68 A. R. Woll, D. H. Bilderback, S. Gruner, N. Gao, R. Huang, C. Bisulca and J. Mass, *MRS Online Proc. Libr.*, 2004, **852**, 65–74.
69 C. Conti, A. Botteon, C. Colombo, M. Realini, P. Matousek, P. Vandenabeele, B. Laforce, B. Vekemans and L. Vincze, *Anal. Methods*, 2018, **10**, 3837–3844.
70 F. C. Izzo, M. Kratter, A. Nevin and E. Zendri, *ChemistryOpen*, 2021, **10**, 904–921.
71 D. Ergenç, M. F. La Russa, S. A. Ruffolo, R. Fort and A. L. Sánchez Montes, *Eur. Phys. J. Plus*, 2018, **133**, 355.
72 C. Germinario, I. Francesco, M. Mercurio, A. Langella, D. Sali, I. Kakoulli, A. De Bonis and C. Grifa, *Eur. Phys. J. Plus*, 2018, **133**, 359.
73 A. Duran and J. L. Perez-Rodriguez, *Vib. Spectrosc.*, 2020, **111**, 103153.
74 P. Noble, in *Metal soaps in art: conservation and research*, ed. F. Casadio, K. Keune, P. Noble, A. Van Loon, E. Hendriks, S. A. Centeno and G. Osmond, Springer, Cham, 2019, pp. 1–22.
75 F. Gabrieli, F. Rosi, A. Vichi, L. Cartechini, L. Pensabene Buemi, S. G. Kazarian and C. Miliani, *Anal. Chem.*, 2017, **89**, 1283–1289.
76 C. Higgitt, M. Spring and D. Saunders, in *National Gallery Technical Bulletin*, 2003, National Gallery Company Limited, London, vol. 24, pp. 75–95.
77 F. Casadio, K. Keune, P. Noble, A. Van Loon, E. Hendriks, S. A. Centeno, G. Osmond, *Metal soaps in art: conservation and research*, Springer, Cham, 2019.
78 M. Spring, C. Ricci, D. A. Peggie and S. G. Kazarian, *Anal. Bioanal. Chem.*, 2008, **392**, 37–45.
79 N. Salvadó, S. Butí, J. Nicholson, H. Emerich, A. Labrador and T. Pradell, *Talanta*, 2009, **79**, 419–428.
80 N. Salvadó, S. Butí, M. Cotte, G. Cinque and T. Pradell, *Appl. Phys. A*, 2013, **111**, 47–57.
81 L. Robinet and M.-C. Corbeil-a, *Stud. Conserv.*, 2003, **48**, 23–40.
82 M. B. Christiansen, E. Baadsgaard, J. Sanyova and K. P. Simonsen, *Heritage Sci.*, 2017, **5**, 39.
83 J. J. Hermans, K. Keune, A. van Loon and P. D. Iedema, *J. Anal. At. Spectrom.*, 2015, **30**, 1600–1608.
84 J. Hermans and K. Helwig, *Appl. Spectrosc.*, 2020, **74**, 1505–1514.
85 R. Mazzeo, S. Prati, M. Quaranta, E. Joseph, E. Kendix and M. Galeotti, *Anal. Bioanal. Chem.*, 2008, **392**, 65–76.
86 E. J. Henderson, K. Helwig, S. Read and S. M. Rosendahl, *Heritage Sci.*, 2019, **7**, 71.
87 M. B. Christiansen, M. A. Sørensen, J. Sanyova, J. Bendix and K. P. Simonsen, *Spectrochim. Acta, Part A*, 2017, **175**, 208–214.
88 Z. Kaszowska, K. Malek, M. Pańczyk and A. Mikołajska, *Vib. Spectrosc.*, 2013, **65**, 1–11.
89 L. Baij, J. J. Hermans, K. Keune and P. Iedema, *Angew. Chem., Int. Ed.*, 2018, **57**, 7351–7354.

90 L. Baij, J. J. Hermans, K. Keune and P. D. Iedema, *Macromolecules*, 2018, **51**, 7134–7144.
91 R. Chércoles Asensio, M. San Andrés Moya, J. M. de la Roja and M. Gómez, *Anal. Bioanal. Chem.*, 2009, **395**, 2081–2096.
92 P. A. Hayes, S. Vahur and I. Leito, *Spectrochim. Acta, Part A*, 2014, **133**, 207–213.
93 L. Ortiz-Herrero, I. Cardaba, S. Setien, L. Bartolomé, M. L. Alonso and M. I. Maguregui, *Talanta*, 2019, **205**, 120114.
94 E. Possenti, C. Colombo, M. Realini, C. L. Song and S. G. Kazarian, *Anal. Bioanal. Chem.*, 2021, **413**, 455–467.
95 A. Vichi, G. Eliazyan and S. G. Kazarian, *ACS Omega*, 2018, **3**, 7150–7157.
96 R. L. Crawford, *Lignin Biodegradation and Transformation*, John Wiley & Sons, New York, 1981.
97 D. M. Updegraff, *Anal. Biochem.*, 1969, **32**, 420–424.
98 Y. Maréchal and H. Chanzy, *J. Mol. Struct.*, 2000, **523**, 183–196.
99 B. Hinterstoisser, M. Akerholm and L. Salmén, *Carbohydr. Res.*, 2001, **334**, 27–37.
100 F. Xu, J. Yu, T. Tesso, F. Dowell and D. Wang, *Appl. Energy*, 2013, **104**, 801–809.
101 K. Fackler, J. Stevanic, T. Ters, B. Hinterstoisser, M. Schwanninger and L. Salmén, *Holzforschung*, 2011, **65**, 411–420.
102 V. Hospodarova, E. Singovszka and N. Stevulova, *Am. J. Anal. Chem.*, 2018, **09**, 303–310.
103 Y. Yan, C. Wen, M. Jin, L. Duan, R. Zhang, C. Luo, J. Xiao, Z. Ye, B. Gao, P. Liu and Y. Tang, *Chem. Res. Chin. Univ.*, 2019, **35**, 586–591.
104 M. Åkerholm, B. Hinterstoisser and L. Salmén, *Carbohydr. Res.*, 2004, **339**, 569–578.
105 M. Nelson and R. T. O'Connor, *J. Appl. Polym. Sci.*, 1964, **8**, 1311–1324.
106 J. Široký, R. S. Blackburn, T. Bechtold, J. Taylor and P. White, *Cellulose*, 2010, **17**, 103–115.
107 A. Kljun, T. A. S. Benians, F. Goubet, F. Meulewaeter, J. P. Knox and R. S. Blackburn, *Biomacromolecules*, 2011, **12**, 4121–4126.
108 R. Kumar, V. Kumar and V. Sharma, *Spectrochim. Acta, Part A*, 2017, **170**, 19–28.
109 F. M. Udriștioiu, I. G. Tănase, A. A. Bunaciu and H. Y. Aboul-Enein, *Appl. Spectrosc. Rev.*, 2012, **47**, 550–570.
110 G. Adami, A. Gorassini, E. Prenesti, M. Crosera, E. Baracchini and A. Giacomello, *Microchem. J.*, 2016, **124**, 96–103.
111 S. Bjarnestad and O. Dahlman, *Anal. Chem.*, 2002, **74**, 5851–5858.
112 K. K. Pandey, *Polym. Degrad. Stab.*, 2005, **90**, 9–20.
113 D. Hunter, *Papermaking: The History and Technique of an Ancient Craft, Dover republications*, New York, 1943.
114 A. Gorassini, P. Calvini and A. Baldin, presented in part at *CMA4CH Meeting 2nd International Symposium on Multivariate Analysis and Chemometry Applied to Environment and Cultural Heritage*, Italy, 2008.
115 V. Librando, Z. Minniti and S. Lorusso, *Conserv. Sci. Cult. Heritage*, 2011, **11**, 249–268.
116 H. Loveday, *Islamic Paper: A Study of the Ancient Craft*, Don Baker Memorial Fund, London, 2001.
117 H. Mahgoub, T. Bardon, D. Lichtblau, T. Fearn and M. Strli, *Heritage Sci.*, 2016, **4**, 1–14.
118 J. M. Bloom, in *Mobilities of Knowledge*, ed. H. Jöns, P. Meusburger and M. Heffernan, Springer International Publishing, Cham, 2017, pp. 51–66.
119 N. Proietti, G. Roselli, D. Capitani, C. Pettinari, S. Pucciarelli, S. Basileo and F. Scognamiglio, *J. Cult. Heritage*, 2020, **42**, 8–18.
120 J. Needham and T. Tsuen-Hsuin, *Science and Civilisation in China: Volume 5, Chemistry and Chemical Technology, Part 1, Paper and Printing*, Cambridge University Press, 1985.
121 Y. Luo, J. Chen, C. Yang and Y. Huang, *Heritage Sci.*, 2019, **7**, 61.
122 L. Wei, W. Chen, G. Jin, Z. Guo, Y. Wang, B. Kang, N. Wang, A. Gu, Y. Zhang and Y. Lei, *Heritage Sci.*, 2018, **6**, 26.
123 C. Ricci, S. Bloxham and S. G. Kazarian, *J. Cult. Heritage*, 2007, **8**, 387–395.
124 E. Imperio, G. Giancane and L. Valli, *Anal. Chem.*, 2013, **85**, 7085–7093.
125 M. Tungol and A. Montaser, *J. Forensic Sci.*, 1991, **36**, 1027–1043.
126 M. W. Tungol, E. G. Bartick, and A. Montaser, in *Practical Guide to Infrared Microspectroscopy*, ed. H. J. Humecki, Taylor & Francis, 1995, pp. 245–285.
127 J. Chae, in *Conservation of Papers and Textiles, National Research Institute of Cultural Heritage*, South Korea, 2012, pp. 262–279.
128 M. Kwiatkowska, R. Pełech, A. Jędrzejewska, D. Moszyński and I. Pełech, *Polymers*, 2020, **12**, 308.
129 M. Porubská, O. Szöllős, A. Kóňová, I. Janigová, M. Jašková, K. Jomová and I. Chodák, *Polym. Degrad. Stab.*, 2012, **97**, 523–531.
130 P. Peets, K. Kaupmees, S. Vahur and I. Leito, *Heritage Sci.*, 2019, **7**, 93.
131 T. Akyuz, S. Akyuz, K. Balci and A. Gulec, *J. Cult. Heritage*, 2017, **25**, 180–184.
132 L. Liu, D. Gong, Z. Yao, L. Xu, Z. Zhu and T. Eckfeld, *Heritage Sci.*, 2019, **7**, 77.
133 Y. Gong, C. Qiao, B. Zhong, J. Zhong and D. Gong, *Heritage Sci.*, 2020, **8**, 13.
134 I. Petroviciu, I. Teodorescu, F. Albu, M. Virgolici, E. Nagoda and A. Medvedovici, *Heritage Sci.*, 2019, **7**, 15.
135 V. Raditoiu, I. E. Chican, A. Raditoiu, I. Fierascu, R. C. Fierascu and P. Fotea, in *VR Technologies in Cultural Heritage*, ed. M. Duguleană, M. Carrozzino, M. Gams, I. Tanea, Springer, Cham, 2019, pp. 3–9.
136 T. Learner, *Analysis of Modern Paints*, Getty Conservation Institute, Getty Publications, Los Angeles, 2004.
137 M. Coughlin and A. M. Seeger, in *Plastics: looking at the future and learning from the past*, ed. B. Keneghan and E. Louise, Archetype, London, 2007, pp. 23–25.

138 J. A. Reilly, *J. Am. Inst. Conserv.*, 1991, **30**, 145–162.
139 Y. Shashoua, *Conservation of Plastics: Materials Science, Degradation and Preservation*, Elsevier/Butterworth-Heinemann, Amsterdam, 2008.
140 Y. Shashoua and C. Ward, in *Resins : ancient and modern*, ed. M. M. Wright and J. Townsend, Scottish Society for Conservation & Restoration, Edinburgh, 1995, pp. 33–37.
141 D. Saviello, L. Toniolo, S. Goidanich and F. Casadio, *Microchem. J.*, 2016, **124**, 868–877.
142 M. Picollo, G. Bartolozzi, C. Cucci, M. Galeotti, V. Marchiafava and B. Pizzo, *Appl. Spectrosc.*, 2014, **68**, 389–396.
143 C. Cucci, G. Bartolozzi, V. Marchiafava, M. Picollo and E. Richardson, *Microchem. J.*, 2016, **124**, 889–897.
144 T. B. van Oosten, in *Contributions to conservation*, ed. J. A. Mosk and N. Tennent, James and James, London, 2002, pp. 87–95.
145 S. Blank, *Stud. Conserv.*, 1990, **35**, 53–63.
146 P. B. Hatchfield, *Pollutants in the Museum Environment: Practical Strategies for Problem Solving in Design, Exhibition and Storage*, Archetype, London, 2002.
147 D. Littlejohn, R. A. Pethrick, A. Quye and J. M. Ballany, *Polym. Degrad. Stab.*, 2013, **98**, 416–424.
148 M. Edge, N. S. Allen, M. Hayes, P. N. K. Riley, C. V. Horie and J. Luc-Gardette, *Eur. Polym. J.*, 1990, **26**, 623–630.
149 I. R. Ahmad, D. Cane, J. H. Townsend, C. Triana, L. Mazzei and K. Curran, *Polym. Degrad. Stab.*, 2020, **172**, 109050.
150 P. Bussière, J. Gardette and S. Thérias, *Polym. Degrad. Stab.*, 2014, **107**, 246–254.
151 J. Bell, P. Nel and B. Stuart, *Heritage Sci.*, 2019, **7**, 95.
152 F. Bressan, R. Bertani, C. Furlan, F. Simionato and S. Canazza, *J. Cult. Heritage*, 2016, **18**, 313–320.
153 S. Hobaica, *J. Appl. Polym. Sci.*, 2013, **128**, 1962–1973.
154 R. Hess, *ARSC J.*, 2008, **39**, 240.
155 S. Nunes, F. Ramacciotti, A. Neves, E. M. Angelin, A. M. Ramos, É. Roldão, N. Wallaszkovits, A. A. Armijo and M. J. Melo, *Heritage Sci.*, 2020, **8**, 33.
156 H. F. Mark, in *Encyclopedia of Polymer Science and Technology*, vol. 4, Wiley, 2011, pp. 697–698.
157 É. C. T. C. Roldão, *PhD thesis*, Universidade NOVA de Lisboa, Portugal, 2018.
158 M. B. Wiggins, E. Heath, K. S. Booksh and J. Alcántara-García, *Appl. Spectrosc.*, 2019, **73**, 1255–1264.
159 100-year paper natural aging project, **https://www.loc.gov/preservation/scientists/projects/100-yr_nat_aging.html**.
160 A. Royaux, I. Fabre-Francke, N. Balcar, G. Barabant, C. Bollard, B. Lavédrine and S. Cantin, *Polym. Degrad. Stab.*, 2017, **137**, 109–121.
161 T. Lamhasni, H. El-Marjaoui, A. El Bakkali, S. A. Lyazidi, M. Haddad, A. Ben-Ncer, F. Benyaich, A. Bonazza and M. Tahri, *Chemosphere*, 2019, **225**, 517–523.
162 M. F. La Russa, V. Comite, N. Aly, D. Barca, P. Fermo, N. Rovella, F. Antonelli, E. Tesser, M. Aquino and S. A. Ruffolo, *Eur. Phys. J. Plus*, 2018, **133**, 370.
163 M. F. La Russa, P. Fermo, V. Comite, C. M. Belfiore, D. Barca, A. Cerioni, M. De Santis, L. F. Barbagallo, M. Ricca and S. A. Ruffolo, *Sci. Total Environ.*, 2017, **593–594**, 297–309.
164 G. E. De Benedetto, R. Laviano, L. Sabbatini and P. G. Zambonin, *J. Cult. Heritage*, 2002, **3**, 177–186.
165 R. M. Ion, I. Dumitriu, R. C. Fierascu, M.-L. Ion, S. F. Pop, C. Radovici, R. I. Bunghez and V. I. R. Niculescu, *J. Therm. Anal. Calorim.*, 2011, **104**, 487–493.
166 S. Centeno, V. Williams, N. Little and R. Speakman, *Vib. Spectrosc.*, 2012, **58**, 119–124.
167 M. Lettieri, *Vib. Spectrosc.*, 2015, **76**, 48–54.
168 L. Medeghini, S. Mignardi, C. De Vito and A. M. Conte, *Microchem. J.*, 2016, **125**, 224–229.
169 A. E. Lavat, M. C. Grasselli and J. E. Tasca, *Ceram. Int.*, 2007, **33**, 1111–1117.
170 M. Vilarigues and R. C. da Silva, *Appl. Phys. A*, 2004, **79**, 373–378.
171 D. Thickett and B. Pretzel, *Heritage Sci.*, 2020, **8**, 5.
172 S. A. MacDonald, C. R. Schardt, D. J. Masiello and J. H. Simmons, *J. Non-Cryst. Solids*, 2000, **275**, 72–82.
173 V. C. Farmer, *The Infrared Spectra of Minerals*, Mineralogical Society of Great Britain and Ireland, 1974.
174 J. A. Gadsden, *Infrared Spectra of Minerals and Related Inorganic Compounds*, Butterworths, 1975.
175 J. R. Ferraro and S. R. Laboratories, *The Sadtler Infrared Spectra Handbook of Minerals and Clays*, Sadtler, 1982.
176 B. Price, J. Carlson and R. Newman, in *Postprints IRUG2 at the V&A*, ed. B. Pretzel, Victoria & Albert Museum, London, 1998, pp. 103–126.
177 D. Barilaro, G. Barone, V. Crupi, M. G. Donato, D. Majolino, G. Messina and R. Ponterio, *J. Mol. Struct.*, 2005, **744–747**, 827–831.
178 L. Maritan, L. Nodari, C. Mazzoli, A. Milano and U. Russo, *Appl. Clay Sci.*, 2006, **31**, 1–15.
179 L. Rampazzi, A. Andreotti, I. Bonaduce, M. P. Colombini, C. Colombo and L. Toniolo, *Talanta*, 2004, **63**, 967–977.
180 P. Maravelaki-Kalaitzaki, *Anal. Chim. Acta*, 2005, **532**, 187–198.
181 E. Possenti, C. Colombo, M. Realini, C. L. Song and S. G. Kazarian, *Anal. Chem.*, 2021, **93**, 14635–14642.
182 İ. Tarhan, İ. Işık and B. Söğüt, *Microchem. J.*, 2021, **162**, 105852.
183 X. Zhou, D. Liu, H. Bu, L. Deng, H. Liu, P. Yuan, P. Du and H. Song, *Solid Earth Sci.*, 2018, **3**, 16–29.
184 S. Vahur, L. Kiudorv, P. Somelar, J.-M. Cayme, M. D. C. Retrato, R. J. Remigio, V. Sharma, E. Oras and I. Leito, *Anal. Bioanal. Chem.*, 2021, **413**, 6535–6550.
185 N. J. Harrick and K. H. Beckmann, in *Characterization of Solid Surfaces*, ed. P. F. Kane, and G. B. Larrabee, Springer, Boston, 1974.
186 T. Frosch, K. L. A. Chan, H. C. Wong, J. T. Cabral and S. G. Kazarian, *Langmuir*, 2010, **26**, 19027–19032.
187 A. Vichi, *PhD thesis*, Imperial College London, 2018.
188 P. Nel, C. Lonetti, D. Lau, K. Tam and R. S. Sloggett, *Vib. Spectrosc.*, 2010, **53**, 64–70.

189 E. Noake, D. Lau and P. Nel, *Heritage Sci.*, 2017, **5**, 3.
190 E. M. Angelin, S. F. de Sá, I. Soares, M. E. Callapez, J. L. Ferreira, M. J. Melo, M. Bacci and M. Picollo, *Appl. Spectrosc.*, 2021, **75**, 818–833.
191 F. Pozzi, A. Rizzo, E. Basso, E. M. Angelin, S. F. de Sá, C. Cucci and M. Picollo, in *Portable Spectroscopy and Spectrometry Volume 2, Applications*, ed. R. A. Crocombe, P. E. Leary and B. W. Kammrath, Wiley, 2021, pp. 499–522.
192 M. Unger, E. Mattson, C. Schmidt Patterson, Z. Alavi, D. Carson and C. J. Hirschmugl, *Appl. Phys. A*, 2013, **111**, 135–145.
193 B. A. Price, B. Pretzel and S. Q. Lomax, *Infrared and Raman Users Group Spectral Database*, 2014, **http://www.irug.org**.
194 M. Caccia, L. Bonizzoni, M. Martini, R. Fontana, V. Villa and A. Galli, *Appl. Spectrosc.*, 2021, **75**, 274–286.
195 R. A. Crocombe, *Appl. Spectrosc.*, 2018, **72**, 1701–1751.